IEEE Access
Multidisciplinary ⋮ Rapid Review ⋮ Open Access Journal

Received February 5, 2022, accepted March 13, 2022, date of publication March 16, 2022, date of current version March 24, 2022.

Digital Object Identifier 10.1109/ACCESS.2022.3159813

Numerical Simulations of Vaccination and Wolbachia on Dengue Transmission Dynamics in the Nonlinear Model

PREM JUNSAWANG[1], SAMINA ZUHRA[2], ZULQURNAIN SABIR[3], MUHAMMAD ASIF ZAHOOR RAJA[4], MUHAMMAD SHOAIB[5], THONGCHAI BOTMART[6], AND WAJAREE WEERA[6]

[1]Department of Statistics, Faculty of Science, Khon Kaen University, Khon Kaen 40002, Thailand
[2]Department of Computing, Abasyn University, Peshawar 25000, Pakistan
[3]Department of Mathematics and Statistics, Hazara University, Mansehra 21120, Pakistan
[4]Future Technology Research Center, National Yunlin University of Science and Technology, Douliou, Yunlin 64002, Taiwan
[5]Department of Mathematics, COMSATS University Islamabad, Attock Campus, Attock 43600, Pakistan
[6]Department of Mathematics, Faculty of Science, Khon Kaen University, Khon Kaen 40002, Thailand

Corresponding author: Thongchai Botmart (thongbo@kku.ac.th)

This work was supported by the NSRF through the Program Management Unit for Human Resources & Institutional Development, Research and Innovation under Grant B05F640088.

ABSTRACT In this study, it is indicated that the world can get rid of the dengue virus by using vaccines and Wolbachia. In many findings, it is observed that Wolbachia therapy is efficacious in those regions that display the minimal to moderate the transmission level. On the contrary, vaccination is highly successful when used in serologically persons and places with large transmission levels. The resilience of stochastic methodology based on the numerical computing schemes will be used to exploit the artificial neural networks (ANNs) modelling legacy, as well as the metaheuristic intelligence using the hybrid of global and local search schemes thru genetic algorithms (GAs) and active-set method (ASA). The combination of both strategies is used to manage the numerical therapies of the mathematical form of the dengue model. The optimal control results through GA-ASA can be retrieved by offering an error-based fitness function generated for dengue model represented via nonlinear systems of equations. The acquired findings are compared to the Adams numerical results to ensure that the suggested stochastic system is accurate. For determining convergence, the training contours are based on various contact rate values. Furthermore, the statistical achievements of the suggested stochastic scheme to solve the novel developed dengue model, which demonstrate the stability and dependability of the dynamical system scheme.

INDEX TERMS Dengue model, vaccination, Wolbachia treatment, genetic algorithm, active set algorithm.

I. INTRODUCTION

Dengue fever, sometimes known as ''tropical flu'', is a viral spreading infection by Aedes mosquitoes. There are four dominant prevalent isoforms (DEN-1, DEN-2, DEN-3, and DEN-4) of this virus globally [1]. The existence of the Aedes species in various Cameroonian locations is reported in [2], whereas others show that this mosquito only attacks daytime [3]. Females' mosquito, mostly Aedes aegypti to a smaller degree carry dengue virus. Each serotype can cause yellow fever, Chikungunya, dengue shock syndrome, and Ebola infections. Dengue fever affects about three billion people around the world, making it a major global public health issue. In high-endemicity urban and suburban regions, this virus is responsible for extremely high mobility and mortality [4]. Dengue fever has increased by 30 times globally during 1960 and 2010, owing to rising population growth, global climate change, rapid urbanization, ineffective mosquito control, extensive air transport, and a lack of access to health facilities. Dengue endemic areas have a population of 2.5 billion people, with around 400 million illnesses each year and a fatality rate of 5–20 percent in some places. Dengue fever is a disease that affects over 100 countries worldwide [5]. Different types of dengue vaccines are under observations comprising Inactivated vaccine, live-attenuated vaccine, DNA vaccine, and viral vectored vaccine, etc. [6].

The associate editor coordinating the review of this manuscript and approving it for publication was Gang Mei.

They work principally by boosting immunogenicity to the E protein and non-structural protein 1 (NS1) of the dengue virus (DENV) [7]. Researching the immunogenicity to DENV can aid in the development of an efficient dengue vaccination strategy [8]. However, the prevalence of four immunologically different dengue virus serotypes, all potentially of generating cross-reactive and disease-enhancing antibody responses against with the three remaining sterotypes, has made the production of a dengue vaccine a difficult process [9]. Scientifically, theoretical calculation of mosquito density reduction is vital, and mosquito density decreases by half on the borders in the region of operations. Ross [10] proposed the concept of mosquito density reduction through the construction of mathematical models several decades earlier.

In recent years, the application of mathematical models to the study of infectious disease epidemic spread has benefited the field of public health in general. For dengue virus propagation, mathematical epidemiological investigations of interaction models involving host–vector and human populations have been developed [11]–[14]. Many dengue mathematical models have been constructed to evaluate the efficiency of Vaccine and Wolbachia intervention in lowering dengue transmission. They discovered that Vaccine and Wolbachia could lower the frequency of dengue cases by up to 80%, especially in areas where propagation is low to moderate [15]–[17]. To observe the heterogeneity and dispersing effects of dengue, mathematical models based on the life cycle and diffusion of mosquitos, as well as geographic heterogeneity of mosquitos, have been constructed. Furthermore, diffusion approaches are used when space is treated as a continual component [18]–[20].

Even though various mathematical models have been developed to examine dengue groove in the presence of vaccination and Wolbachia, rare have considered the combination of the two techniques. It is critical to analyze the results of both approaches independently and collectively. The objective of this research is to explore a mathematical model of vaccination and Wolbachia used for dengue transmission and dispersal and its analysis in the form of simulation solutions to assist in understanding dynamic behavior using a stochastic technique. Exploring the prospect of fixing linear/nonlinear systems using the high predictive capabilities of feedforward artificial neural networks (ANNs) optimized with the combined capabilities of local/global search methods is a significant potential of meta-heuristic computing paradigm based on stochastic approach [21]–[23]. Soft computing techniques reported in different diseases such as Convolution neural networks for analysis of plant diseases [24], [25], for COVID-19 disease [26]–[29], artificial neural networks for tuberculosis [30], for forecasting disease [31], for skin diseases [32], chest disease [33], for diagnosis of kidney stone diseases [34], respiratory disease [35], for HIV infection [36], to analyze influenza disease model [37] and for stomach model [38]. In the field of fluid mechanic, ANNs successfully tightened the claws as these techniques have been proved best for nonlinear complicated flow system [39]–[43]. Forecasting and finance require soft computing for rapid marketing [44], [45].

It is investigated that the vaccination and Wolbachia have been used to prevent the dengue spread. Wolbachia possesses properties that differ from the insecticide-based technique, which could have an impact on disease transmission dynamics. We shall demonstrate the effectiveness of these tactics separately or jointly after simulating the model. The goal of the research is to find the numerical solutions via artificial neural network understanding of the strategy's effectiveness, hence a single serotype dengue model will suffice.

Key procedure is as under

- The effectiveness is validated using statistical evaluations of the dengue nonlinear system based on differential equations on numerous ANN-GA-ASA trials in terms of mean absolute deviation, semi-interquartile range and 'Theil's inequality coefficient.'
- Aside from the accurate results for the Dengue nonlinear differential model with initial conditions, additional valuable features include ease of understanding, faster operation, stability, broad applicability, and robustness.

The paper is arranged into 4 sections. Section 2 comprises the formulation of dengue model and its parameters along values. Section 3 shows the ANN-GA-ASA methodology for solving the dengue, as well as the mathematical form of the statistical operators. Section 4 contains the summary of the findings.

II. FORMULATION OF MATHEMATICAL MODEL

A predictable mathematical model is constructed for the dengue treatment that covers Wolbachia and vaccinated presented by Nedii *et al.* [17]. In this model the attacking agent (mosquito) and effected agent human are distributed into two separate compartments. Attacking agent population are distributed into Aquatic A, Susceptible S, Exposed E and Infectious I, whereas human population are distributed into Susceptible S_H, Vaccinated V_H, Exposed E_H, Infectious I_H and Recovered R_H.

The purpose of this paper is to get a broad understanding of the potential efficacy of vaccines and Wolbachia. The basic assumptions used to build the model are as follows:

- Mosquitoes have no recovery class because they are contagious for the remainder of their lives.
- It is sufficient to utilize a single serotype dengue model.

When susceptible individuals are attacked by contaminated non-Wolbachia and Wolbachia-carrying mosquitoes at a rate of λ_n and λ_W, respectively, they become infected. The human species are injected at a rate of V_H. Vaccinated people, on the other hand, are exposed to dengue when the vaccine loses its efficiency at a rates $(1-\varepsilon)$ and they are struck by diseased non-Wolbachia and Wolbachia-carrying mosquitoes at rates λ_n and λ_W, respectively. We consider diminishing immunity, which occurs at a rate of φ_h, as well as randomized bulk vaccination. The mathematical constrain for disease model

TABLE 1. Brief description with symbols and their numerical values per day as unite [17].

Symbols	Description	Values (day^{-1})
β	Birth rate	$1/(66.38\times365)$
μ_H	Natural death rate	$1/(66.38\times365)$
p	Vaccinated rate	0.20
ε	Vaccine efficacy	0.538
φ	Waning immunity	0.10
ω	Maternal transmission	0.90
b_N	Non-wolbachia biting rate	0.63
b_W	Wolbachia biting rate	0.95 of b_N
μ_N	Adult mosquito death rate	0.070
μ_{AW}	Aquatic death rate	0.070
μ_W	Wolbachia death rate	1.1 of μ_N
τ_W	Maturation rate of Wolbachia	0.10
τ_N	Maturation rate on non-Wolbachia	1.25
τ_W	Maturation rate on Wolbachia	0.10
γ_H	Exposed to infectious human progression rate	0.182
γ_N	Exposed to infectious non-Wolbachia progression rate	0.10
T_N	Transmission Probability	0.2614
γ_W	Exposed to infectious progression rate	0.10
ρ_N	Non-Wolbachia reproduction rate	1.25
ρ_W	Wolbachia reproduction rate	0.95 of ρ_N
α	Recovery rate	0.25
T_{HW}	Infectious W to human transfer probability	0.50 of T_N
λ_n	Non-Wolbachia carrying mosquitoes rate	0.1647
λ_w	Wolbachia carrying mosquitoes rate	0.95
I_N	Non-Wolbachia infectious rate	0.3
I_W	Wolbachia infectious rate	0.2

is given as:

$$
\begin{aligned}
S_H'(t) &= \beta N_H - (\lambda_n + p + \lambda_w + \mu_H)S_H(t) + \varphi V_H(t),\\
V_H'(t) &= pS_H - (1-\varepsilon)V_H(t)(\lambda_n + \lambda_w) - V_H(t)(\varphi + \mu_h),\\
E_H'(t) &= (\lambda_n + \lambda_w) S_H(t) + (1-\varepsilon)V_H(t)(\lambda_n + \lambda_w)\\
&\quad - E_H(t)(\gamma_H + \mu_H),\\
I_H'(t) &= \gamma_H E_H(t) - \alpha I_H(t) - \mu_H S_H(t),\\
R_H'(t) &= \alpha I_H(t) - \mu_H R_H(t),\\
A_N'(t) &= \frac{1}{2(F_N+F_W)}\rho_N F_N^2\left(1 - \frac{(A_N(t)+A_W(t))}{K}\right)\\
&\quad - A_N(t)(\tau_N + \mu_{NA}),\\
S_N'(t) &= \frac{A_N(t)\tau_N}{2} + (1-\omega)\frac{A_N(t)\tau_N}{2} - \frac{T_N b_N I_H(t) S_N(t)}{N_H}\\
&\quad - \mu_N S_N(t),\\
E_N'(t) &= \frac{T_N b_N I_H(t) S_N(t)}{N_H} - \gamma_N E_N(t) - \mu_N E_N(t),\\
I_N'(t) &= \gamma_N E_N(t) - \mu_N I_N(t),\\
A_W'(t) &= \frac{\rho_W F_W}{2K}(K - (A_N(t) + A_W(t)))\\
&\quad - A_W(t)(\mu_{WA} - \tau_W),\\
S_W'(t) &= \frac{\omega A_W(t)\tau_W}{2} - \frac{S_W(t)}{N_H}(\mu_W + b_W T_N I_H(t)),\\
E_W'(t) &= \frac{b_W T_N I_H(t) S_W(t)}{N_H} - \gamma_W E_W(t) - \mu_W E_W(t),\\
I_W'(t) &= \gamma_W E_W(t) - \mu_W I_W(t), \qquad (1)
\end{aligned}
$$

where

$$\lambda_n = \frac{T_N b_N I_N}{N_H}, \quad \lambda_W = \frac{b_W T_{HW} I_W}{N_H}.$$

We calculate the basic reproduction number, which is the average number of new viruses created by one infected adult in a completely vulnerable group, using the notion of the next generation matrix. In the absence of modifications, the basic reproduction number is,

$$R_A = \sqrt{\frac{T_N^2 b_N^2 \gamma_N \gamma_H S_N}{\mu_N N_H (\alpha + \mu_H)(\gamma_H + \mu_H)(\gamma_N + \mu_N)}}$$

III. METHODOLOGY

For addressing the nonlinear mathematical dengue model, the developed structure of ANNs utilizing GA-ASA optimum is provided in two steps, as follows:

- The fitness function design is described for the ANNs parameters.
- The hybrid combination of GA-ASA provides vital settings for optimizing fitness function.

A. STRUCTURE OF ANNS

This section contains the mathematical formulas for solving each class of the nonlinear Causative Agent Prevention Virus (dengue model). The functions of the nonlinear dengue model are respectively represented as $S_H, V_H, E_H, I_H, R_H, A_N, S_N, E_N, I_N, A_W, S_W, E_W$, and I_W given as (2), shown at the bottom of the next page.

$\boldsymbol{W}$ signifies the unidentified weights in the above system, given as:

$$
\begin{aligned}
\boldsymbol{W} &= [\boldsymbol{W}_{S_H}, \boldsymbol{W}_{V_H}, \boldsymbol{W}_{E_H}, \boldsymbol{W}_{I_H}, \boldsymbol{W}_{R_H}, \boldsymbol{W}_{S_N}, \boldsymbol{W}_{E_N},\\
&\quad \boldsymbol{W}_{A_N}, \boldsymbol{W}_{I_N}, \boldsymbol{W}_{A_W}, \boldsymbol{W}_{S_W}, \boldsymbol{W}_{E_W}, \boldsymbol{W}_{I_W}], \text{ for}\\
\boldsymbol{W}_{S_H} &= [\boldsymbol{k}_{S_H}, \boldsymbol{\omega}_{S_H}, \boldsymbol{c}_{S_H}], \quad \boldsymbol{W}_{V_H} = [\boldsymbol{k}_{V_H}, \boldsymbol{\omega}_{V_H}, \boldsymbol{c}_{V_H}],\\
\boldsymbol{W}_{E_H} &= [\boldsymbol{k}_{E_H}, \boldsymbol{\omega}_{E_H}, \boldsymbol{c}_{E_H}], \quad \boldsymbol{W}_{I_H} = [\boldsymbol{k}_{I_H}, \boldsymbol{\omega}_{I_H}, \boldsymbol{c}_{I_H}],\\
\boldsymbol{W}_{R_H} &= [\boldsymbol{k}_{R_H}, \boldsymbol{\omega}_{R_H}, \boldsymbol{c}_{R_H}], \quad \boldsymbol{W}_{A_N} = [\boldsymbol{k}_{A_N}, \boldsymbol{\omega}_{A_N}, \boldsymbol{c}_{A_N}],
\end{aligned}
$$

$$\boldsymbol{W}_{S_N} = [\boldsymbol{k}_{S_N}, \boldsymbol{\omega}_{S_N}, \boldsymbol{a}_{S_N}],$$
$$\boldsymbol{W}_{E_N} = [\boldsymbol{k}_{E_N}, \boldsymbol{\omega}_{E_N}, \boldsymbol{c}_{E_N}],$$
$$\boldsymbol{W}_{I_N} = [\boldsymbol{k}_{I_N}, \boldsymbol{\omega}_{I_N}, \boldsymbol{c}_{I_N}], \quad \boldsymbol{W}_{A_W} = [\boldsymbol{k}_{A_W}, \boldsymbol{\omega}_{A_W}, \boldsymbol{c}_{A_W}],$$
$$\boldsymbol{W}_{S_W} = [\boldsymbol{k}_{S_W}, \boldsymbol{\omega}_{S_W}, \boldsymbol{c}_{S_W}], \quad \boldsymbol{W}_{E_W} = [\boldsymbol{k}_{E_W}, \boldsymbol{\omega}_{E_W}, \boldsymbol{c}_{E_W}]$$

and

$$\boldsymbol{W}_{I_W} = [\boldsymbol{k}_{I_W}, \boldsymbol{\omega}_{I_W}, \boldsymbol{c}_{I_W}].$$
$$\boldsymbol{k}_{S_H} = [k_{S_H,1}, k_{S_H,2}, \ldots, k_{S_H,m}],$$
$$\boldsymbol{k}_{V_H} = [k_{V_H,1}, k_{V_H,2}, \ldots, k_{V_H,m}],$$
$$\boldsymbol{k}_{E_H} = [k_{E_H,1}, k_{E_H,2}, \ldots, k_{E_H,m}],$$
$$\boldsymbol{k}_{I_H} = [k_{I_H,1}, k_{I_H,2}, \ldots, k_{I_H,m}],$$
$$\boldsymbol{k}_{R_H} = [k_{R_H,1}, k_{R_H,2}, \ldots, k_{R_H,m}],$$
$$\boldsymbol{k}_{A_N} = [k_{A_N,1}, k_{A_N,2}, \ldots, k_{A_N,m}],$$
$$\boldsymbol{k}_{S_N} = [k_{S_N,1}, k_{S_N,2}, \ldots, k_{S_N,m}],$$
$$\boldsymbol{k}_{E_N} = [k_{E_N,1}, k_{E_N,2}, \ldots, k_{E_N,m}],$$
$$\boldsymbol{k}_{I_N} = [k_{I_N,1}, k_{I_N,2}, \ldots, k_{I_N,m}],$$
$$\boldsymbol{k}_{A_W} = [k_{A_W,1}, k_{A_W,2}, \ldots, k_{A_W,m}],$$
$$\boldsymbol{k}_{S_W} = [k_{S_W,1}, k_{S_W,2}, \ldots, k_{S_W,m}],$$
$$\boldsymbol{k}_{E_W} = [k_{E_W,1}, k_{E_W,2}, \ldots, k_{E_W,m}],$$
$$\boldsymbol{k}_{I_W} = [k_{I_W,1}, k_{I_W,2}, \ldots, k_{I_W,m}],$$
$$\boldsymbol{w}_{S_H} = [w_{S_H,1}, w_{S_H,2}, \ldots, w_{S_H,m}],$$
$$\boldsymbol{w}_{V_H} = [w_{V_H,1}, w_{V_H,2}, \ldots, w_{V_H,m}],$$
$$\boldsymbol{w}_{E_H} = [w_{E_H,1}, w_{E_H,2}, \ldots, w_{E_H,m}],$$
$$\boldsymbol{w}_{I_H} = [w_{I_H,1}, w_{I_H,2}, \ldots, w_{I_H,m}],$$
$$\boldsymbol{w}_{R_H} = , [w_{R_H,1}, w_{R_H,2}, \ldots, w_{R_H,m}],$$
$$\boldsymbol{w}_{A_N} = [w_{A_N,1}, w_{A_N,2}, \ldots, w_{A_N,m}],$$
$$\boldsymbol{w}_{E_N} = [w_{E_N,1}, w_{E_N,2}, \ldots, w_{E_N,m}],$$
$$\boldsymbol{w}_{S_N} = [w_{S_N,1}, w_{S_N,2}, \ldots, w_{S_N,m}],$$
$$\boldsymbol{w}_{I_N} = [w_{I_N,1}, w_{I_N,2}, \ldots, w_{I_N,m}],$$
$$\boldsymbol{w}_{A_W} = [w_{A_W,1}, w_{A_W,2}, \ldots, w_{A_W,m}],$$
$$\boldsymbol{w}_{S_W} = [w_{S_W,1}, w_{S_W,2}, \ldots, w_{S_W,m}],$$
$$\boldsymbol{w}_{I_W} = [w_{I_W,1}, w_{I_W,2}, \ldots, w_{I_W,m}],$$
$$\boldsymbol{w}_{E_W} = [w_{E_W,1}, w_{E_W,2}, \ldots, w_{E_W,m}],$$
$$\boldsymbol{c}_{S_N} = [c_{S_N,1}, c_{S_N,2}, \ldots, c_{S_N,m}],$$
$$\boldsymbol{c}_{S_H} = [c_{S_H,1}, c_{S_H,2}, \ldots, c_{S_H,m}],$$
$$\boldsymbol{c}_{V_H} = [c_{V_H,1}, c_{V_H,2}, \ldots, c_{V_H,m}],$$
$$\boldsymbol{c}_{E_H} = [c_{E_H,1}, c_{E_H,2}, \ldots, c_{E_H,m}],$$
$$\boldsymbol{c}_{I_H} = [c_{I_H,1}, c_{I_H,2}, \ldots, c_{I_H,m}],$$
$$\boldsymbol{c}_{R_H} = [c_{R_H,1}, c_{R_H,2}, \ldots, c_{R_H,m}],$$
$$\boldsymbol{c}_{A_N} = [c_{A_N,1}, c_{A_N,2}, \ldots, c_{A_N,m}],$$
$$\boldsymbol{c}_{E_N} = [c_{E_N,1}, c_{E_N,2}, \ldots, c_{E_N,m}],$$

$$\begin{bmatrix} S_H(t), & V_H(t), & E_H(t), & I_H(t) \\ R_H(t), & A_N(t), & S_N(t), & E_N(t), \\ I_N(t), & A_W(t), & S_W(t), & E_W(t), \\ I_W(t) \end{bmatrix} = \begin{bmatrix} \sum_{i=1}^{m} k_{S_H,i} g(w_{S_H,i}t + c_{S_H,i}), & \sum_{i=1}^{m} k_{V_H,i} g(w_{V_H,i}\tau + c_{V_H,i}), \\ \sum_{i=1}^{m} k_{E_H,i} g(w_{E_H,i}t + c_{E_H,i}), & \sum_{i=1}^{m} k_{I_H,i} g(w_{I_H,i}t + c_{I_H,i}), \\ \sum_{i=1}^{m} k_{R_H,i} g(w_{R_H,k}t + c_{R_H,i}), & \sum_{i=1}^{m} k_{A_N,i} g(w_{A_N,i}t + c_{A_N,i}), \\ \sum_{i=1}^{m} k_{S_N,i} g(w_{S_N,i}t + c_{S_N,i}), & \sum_{i=1}^{m} k_{E_N,i} g(w_{E_N,i}t + c_{E_N,i}), \\ \sum_{i=1}^{m} k_{I_N,i} g(w_{I_N,k}t + c_{I_N,i}), & \sum_{i=1}^{m} k_{A_W,i} g(w_{A_W,i}t + c_{A_W,i}), \\ \sum_{i=1}^{m} k_{S_W,i} g(w_{S_W,i}t + c_{S_W,i}), & \sum_{i=1}^{m} k_{E_W,i} g(w_{E_W,i}t + c_{E_W,i}), \\ \multicolumn{2}{c}{\sum_{i=1}^{m} k_{I_W,i} g(w_{I_W,i}t + c_{I_W,i})} \end{bmatrix},$$

$$\begin{bmatrix} S'_H(t), & V'_H(t), & E'_H(t), & I'_H(t) \\ R'_H(t), & A'_N(t), & S'_N(t), & E'_N(t), \\ I'_N(t), & A'_W(t), & S'_W(t), & E'_W(t), \\ I'_W(t) \end{bmatrix} = \begin{bmatrix} \sum_{i=1}^{m} k_{S_H,i} g'(w_{S_H,i}t + c_{S_H,i}), & \sum_{i=1}^{m} k_{V_H,i} g'(w_{V_H,i}\tau + c_{V_H,i}), \\ \sum_{i=1}^{m} k_{E_H,i} g'(w_{E_H,i}t + c_{E_H,i}), & \sum_{i=1}^{m} k_{I_H,i} g'(w_{I_H,i}t + c_{I_H,i}), \\ \sum_{i=1}^{m} k_{R_H,i} g'(w_{R_H,k}t + c_{R_H,i}), & \sum_{i=1}^{m} k_{A_N,i} g'(w_{A_N,i}t + c_{A_N,i}), \\ \sum_{i=1}^{m} k_{S_N,i} g'(w_{S_N,i}t + c_{S_N,i}), & \sum_{i=1}^{m} k_{E_N,i} g'(w_{E_N,i}t + c_{E_N,i}), \\ \sum_{i=1}^{m} k_{I_N,i} g'(w_{I_N,k}t + c_{I_N,i}), & \sum_{i=1}^{m} k_{A_W,i} g'(w_{A_W,i}t + c_{A_W,i}), \\ \sum_{i=1}^{m} k_{S_W,i} g'(w_{S_W,i}t + c_{S_W,i}), & \sum_{i=1}^{m} k_{E_W,i} g'(w_{E_W,i}t + c_{E_W,i}), \\ \multicolumn{2}{c}{\sum_{i=1}^{m} k_{I_W,i} g'(w_{I_W,i}t + c_{I_W,i})} \end{bmatrix}, \tag{2}$$

$$
\begin{aligned}
\boldsymbol{c}_{I_N} &= [c_{I_N,1},\ c_{I_N,2},\ \ldots,\ c_{I_N,m}],\\
\boldsymbol{c}_{A_W} &= [c_{A_W,1},\ c_{A_W,2},\ \ldots,\ c_{A_W,m}],\\
\boldsymbol{c}_{S_W} &= [c_{S_W,1},\ c_{S_W,2},\ \ldots,\ c_{S_W,m}],\\
\boldsymbol{c}_{E_W} &= [c_{E_W,1},\ c_{E_W,2},\ \ldots,\ c_{E_W,m}],\\
\boldsymbol{c}_{I_W} &= [c_{I_W,1},\ c_{I_W,2},\ \ldots,\ c_{I_W,m}].
\end{aligned}
$$

In the above system, the activation function log-sigmoid $g(\tau) = 1/\left(1 + E\wedge(-\tau)\right)$ is applied given as (3), shown at the bottom of the page.

The GA-ASA techniques are used to optimize an error-based 'fitness function,' which is given as:

$$
e = \sum_{n=1}^{14} e_n, \tag{4}
$$

$$
e_1 = \frac{1}{N}\sum_{i=1}^{N}\Big[(\hat{S}'_H)_i - \beta N_H + (\lambda_n + p + \lambda_w + \mu_H)(\hat{S}_H)_i - \varphi(\hat{V}_H)_i\Big]^2, \tag{5}
$$

$$
e_2 = \frac{1}{N} \times \sum_{i=1}^{N}\Big[(\hat{V}'_H)_i - p(\hat{S}_H)_i + (1-\varepsilon)(\hat{V}_H)_i\,(\lambda_n + \lambda_w) + (\hat{V}_H)_i\,(\varphi + \mu_h)\Big]^2, \tag{6}
$$

$$
e_3 = \frac{1}{N} \times \sum_{i=1}^{N}\Big[(\hat{E}'_H)_i - (\lambda_n + \lambda_w)\,(\hat{S}_H)_i - (1-\varepsilon)(\hat{V}_H(t))_i \times (\lambda_n + \lambda_w) + (\hat{E}_H)_i\,(\gamma_H + \mu_H)\Big]^2, \tag{7}
$$

$$
e_4 = \frac{1}{N}\sum_{i=1}^{N}\Big[(\hat{I}'_H)_i - \gamma_H(\hat{E}_H)_i + \alpha(\hat{I}_H)_i + \mu_H(\hat{S}_H)_i\Big]^2, \tag{8}
$$

$$
\begin{bmatrix}
\hat{S}_H(t), & \hat{V}_H(t), & \hat{E}_H(t), & \hat{I}_H(t)\\
\hat{R}_H(t), & \hat{A}_N(t), & \hat{S}_N(t), & \hat{E}_N(t),\\
\hat{I}_N(t), & \hat{A}_W(t), & \hat{S}_W(t), & \hat{E}_W(t),\\
\hat{I}_W(t) & & &
\end{bmatrix}
=
\begin{bmatrix}
\sum_{i=1}^{m}\frac{k_{S_H,i}}{1+e^{-(w_{S_H,i}t+c_{S_H,i})}}, \sum_{i=1}^{m}\frac{k_{V_H,i}}{1+e^{-(w_{V_H,i}t+c_{V_H,i})}},\\
\sum_{i=1}^{m}\frac{k_{E_H,i}}{1+e^{-(w_{E_H,i}t+c_{E_H,i})}}, \sum_{i=1}^{m}\frac{k_{I_H,i}}{1+e^{-(w_{I_H,i}t+c_{I_H,i})}},\\
\sum_{i=1}^{m}\frac{k_{R_H,i}}{1+e^{-(w_{R_H,i}t+c_{R_H,i})}}, \sum_{i=1}^{m}\frac{k_{A_N,i}}{1+e^{-(w_{A_N,i}t+c_{A_N,i})}},\\
\sum_{i=1}^{m}\frac{k_{S_N,i}}{1+e^{-(w_{S_N,i}t+c_{S_N,i})}}, \sum_{i=1}^{m}\frac{k_{E_N,i}}{1+e^{-(w_{E_N,i}t+c_{E_N,i})}},\\
\sum_{i=1}^{m}\frac{k_{I_N,i}}{1+e^{-(w_{I_N,i}t+c_{I_N,i})}}, \sum_{i=1}^{m}\frac{k_{A_W,i}}{1+e^{-(w_{A_W,i}t+c_{A_W,i})}},\\
\sum_{i=1}^{m}\frac{k_{S_W,i}}{1+e^{-(w_{S_W,i}t+c_{S_W,i})}}, \sum_{i=1}^{m}\frac{k_{E_W,i}}{1+e^{-(w_{E_W,i}t+c_{E_W,i})}},\\
\sum_{i=1}^{m}\frac{k_{I_W,i}}{1+e^{-(w_{I_W,i}t+c_{I_W,i})}}
\end{bmatrix},
$$

$$
\begin{bmatrix}
\hat{S}'_H(t), & \hat{V}'_H(t), & \hat{E}'_H(t), & \hat{I}'_H(t)\\
\hat{R}'_H(t), & \hat{A}'_N(t), & \hat{S}'_N(t), & \hat{E}'_N(t),\\
\hat{I}'_N(t), & \hat{A}'_W(t), & \hat{S}'_W(t), & \hat{E}'_W(t),\\
\hat{I}'_W(t) & & &
\end{bmatrix}
=
\begin{bmatrix}
\sum_{i=1}^{m}\frac{w_{S_H,i}k_{S_H,i}e^{-(w_{S_H,i}t+c_{S_H,i})}}{\left(1+e^{-(w_{S_H,i}t+c_{S_H,i})}\right)^2}, \sum_{i=1}^{m}\frac{w_{V_H,i}k_{V_H,i}e^{-(w_{V_H,i}t+c_{V_H,i})}}{\left(1+e^{-(w_{V_H,i}t+c_{V_H,i})}\right)^2},\\
\sum_{i=1}^{m}\frac{w_{E_H,i}k_{E_H,i}e^{-(w_{E_H,i}t+c_{E_H,i})}}{\left(1+e^{-(w_{E_H,i}t+c_{E_H,i})}\right)^2}, \sum_{i=1}^{m}\frac{w_{I_H,i}k_{I_H,i}e^{-(w_{I_H,i}t+c_{I_H,i})}}{\left(1+e^{-(w_{I_H,i}t+c_{I_H,i})}\right)^2},\\
\sum_{i=1}^{m}\frac{w_{R_H,i}k_{R_H,i}e^{-(w_{R_H,i}t+c_{R_H,i})}}{\left(1+e^{-(w_{R_H,i}t+c_{R_H,i})}\right)^2}, \sum_{i=1}^{m}\frac{w_{E_N,i}k_{E_N,i}e^{-(w_{E_N,i}t+c_{E_N,i})}}{\left(1+e^{-(w_{E_N,i}t+c_{E_N,i})}\right)^2},\\
\sum_{i=1}^{m}\frac{w_{I_N,i}k_{I_N,i}e^{-(w_{I_N,i}t+c_{I_N,i})}}{\left(1+e^{-(w_{I_N,i}t+c_{I_N,i})}\right)^2}, \sum_{i=1}^{m}\frac{w_{A_W,i}k_{A_W,i}e^{-(w_{A_W,i}t+c_{A_W,i})}}{\left(1+e^{-(w_{A_W,i}t+c_{A_W,i})}\right)^2},\\
\sum_{i=1}^{m}\frac{w_{A_N,i}k_{A_N,i}e^{-(w_{A_N,i}t+c_{A_N,i})}}{\left(1+e^{-(w_{A_N,i}t+c_{A_N,i})}\right)^2}, \sum_{i=1}^{m}\frac{w_{S_N,i}k_{S_N,i}e^{-(w_{S_N,i}t+c_{S_N,i})}}{\left(1+e^{-(w_{S_N,i}t+c_{S_N,i})}\right)^2},\\
\sum_{i=1}^{m}\frac{w_{S_W,i}k_{S_W,i}e^{-(w_{S_W,i}t+c_{S_W,i})}}{\left(1+e^{-(w_{S_W,i}t+c_{S_W,i})}\right)^2}, \sum_{i=1}^{m}\frac{w_{E_W,i}k_{E_W,i}e^{-(w_{E_W,i}t+c_{E_W,i})}}{\left(1+e^{-(w_{E_W,i}t+c_{E_W,i})}\right)^2},\\
\sum_{i=1}^{m}\frac{w_{I_W,i}k_{I_W,i}e^{-(w_{I_W,i}t+c_{I_W,i})}}{\left(1+e^{-(w_{I_W,i}t+c_{I_W,i})}\right)^2}
\end{bmatrix}. \tag{3}
$$

$$e_5 = \frac{1}{N}\sum_{i=1}^{N}\left[(\hat{R}'_H)_i - \alpha(\hat{I}_H)_i + \mu_H(\hat{R}_H)_i\right]^2, \tag{9}$$

$$e_6 = \frac{1}{N} \times \sum_{i=1}^{N}\left[(\hat{A}'_N)_i - \frac{1}{2(F_N+F_W)}\rho_N F_N^2 \left(1 - \frac{\left((\hat{A}_N)_i + (\hat{A}_W)_i\right)}{K}\right) + (\hat{A}_N)_i(\tau_N + \mu_{NA})\right]^2, \tag{10}$$

$$e_7 = \frac{1}{N} \times \sum_{i=1}^{N}\left[(\hat{S}'_N)_i - \frac{(\hat{A}_N)_i\tau_N}{2} - (1-\omega)\frac{(\hat{A}_N)_i\tau_N}{2} + \frac{T_N b_N(\hat{I}_H)_i(\hat{S}_N)_i}{N_H} + \mu_N(\hat{S}_N)_i\right]^2, \tag{11}$$

$$e_8 = \frac{1}{N}\sum_{i=1}^{N}\left[(\hat{E}'_N)_i - \frac{T_N b_N(\hat{I}_H)_i(\hat{S}_N)_i}{N_H} + \gamma_N(\hat{E}_N)_i + \mu_N(\hat{E}_N)_i\right]^2, \tag{12}$$

$$e_9 = \frac{1}{N}\sum_{i=1}^{N}\left[(\hat{I}'_N)_i - \gamma_N(\hat{E}_N)_i - \mu_N(\hat{I}_N)_i\right]^2, \tag{13}$$

$$e_{10} = \frac{1}{N}\sum_{i=1}^{N}\left[(\hat{A}'_W)_i - \frac{\rho_W F_W}{2K}\left(K - \left((\hat{A}_N)_i + (\hat{A}_W)_i\right)\right) - (\hat{A}_W)_i(\mu_{WA} - \tau_W)\right]^2, \tag{14}$$

$$e_{11} = \frac{1}{N}\sum_{i=1}^{N}\left[(\hat{S}'_W)_i - \frac{\omega(\hat{A}_W)_i\tau_W}{2} - \frac{(\hat{S}_W)_i}{N_H} \times \left(\mu_W + b_W T_N(\hat{I}_H)_i\right)\right]^2, \tag{15}$$

$$e_{12} = \frac{1}{N}\sum_{i=1}^{N}\left[(\hat{E}'_W) - \frac{b_W T_N(\hat{I}_H)_i(\hat{S}_W)_i}{N_H} - \gamma_W(\hat{E}_W)_i - \mu_W(\hat{E}_W)_i\right]^2, \tag{16}$$

$$e_{13} = \frac{1}{N}\sum_{i=1}^{N}\left[(\hat{I}'_W)_i - \gamma_W(\hat{E}_W)_i + \mu_W(\hat{I}_W)_i\right]^2, \tag{17}$$

$$e_{14} = \frac{1}{13}\begin{bmatrix} ((\hat{S}'_H)_i - I_1)^2 + ((\hat{V}'_H)_i - I_2)^2 + ((\hat{E}'_H)_i - I_3)^2 \\ + ((\hat{I}'_H)_i - I_4)^2 + ((\hat{R}'_H)_i - I_5)^2 + ((\hat{A}'_N)_i - I_6)^2 \\ + ((\hat{S}'_N)_i - I_7)^2 + ((\hat{E}'_N)_i - I_8)^2 + ((\hat{I}'_N)_i - I_9)^2 \\ + ((\hat{A}'_W)_i - I_{10})^2 + ((\hat{S}'_W)_i - I_{11})^2 + ((\hat{E}'_W)_i - I_{12})^2 \\ + ((\hat{I}'_W)_i - I_{13})^2 \end{bmatrix}. \tag{18}$$

where

$$\begin{aligned} &(\hat{S}_H)_i = S_H(t_i), && (\hat{V}_H)_i = V_H(t_i), \\ &(\hat{E}_H)_i = E_H(t_i), && (\hat{I}_H)_i = I_H(t_i), \\ &(\hat{R}_H)_i = R_H(t_i), && (\hat{A}_N)_i = A_N(t_i), \\ &(\hat{S}_N)_i = S_N(t_i), && (\hat{E}_N)_i = E_N(t_i), \\ &(\hat{I}_N)_i = I_N(t_i), && (\hat{A}_W)_i = A_W(t_i), \\ &(\hat{S}_W)_i = S_W(t_i), && (\hat{E}_W)_i = E_W(t_i), \\ &(\hat{I}_W)_i = I_W(t_i). \end{aligned}$$

The quantites $e_1, e_2, e_3 \ldots$ and e_{13} indicate the fitness functions associated to differential system (1), whereas the corresponding initial conditions is represented in e_{14}.

B. OPTIMIZATION PERFORMANCES: GA-ASA

Optimal performance of nonlinear mathematical model of dengue virus with treatment procedure is simulated thru the artificial technique GA-ASA. The genetic algorithm (GA) is a paradigm of abiogenesis introduce by John Holland *et al.* [46]. He was widely credited as being the first one to bring the concept of crossover, mutation and selections in artificial system which are the necessary parts of genetic algorithm arise as problem-solving agent. Since that day, a variety of genetic algorithm versions have now been devised and utilized in a variety of optimization problems, ranging from discrete systems like salesperson travelling problem to continuous systems arise in designation of airfoils in aerospace, from coloring of graph to pattern recognition, and from monetary markets to multi-objective engineering optimization [47]. Many other applications of GA are in biomedical field such as cancer datasets with multi-dimensional [48], categorization of anomalous computed tomography brain tumor images [49], transcriptomic cancer classifier [50], prediction of liver diseases model [51], in transportation field applicable in vehicle routing model and monorail dynamics model [52], [53], in geophysical side for prediction of air blast [54], cloud model [55], and for groundwater flow model [56], and wind power systems [57], etc.

Using the hybridize with the local search technique, quick convergence is achieved by combining global search with any local search approach. As an initial input, the best GA values are assigned. To standardize the variables, the local search active set algorithm is used. In optimization theory, the active set is highly crucial since it decides which constraints will have an impact on the result of optimization. The active set, for instance, specifies the hyperplanes that cross at the solution point while solving a linear programming issue. Here are few contributions that us ASA such that water supply model to manage the flow [58], optimal control issue based on PDE [59], node-based shape optimization [60], and for electrodynamic problems [61].

The constructed ANNs-GA-ASA for the dengue model is illustrated in Figure 2.

TABLE 2. Optimization procedure thru ANN-GA-ASA for dengue mathematical model.

GA **Inputs:** The selection of the chromosomes is $\boldsymbol{W} = [\boldsymbol{k}, \boldsymbol{w}, \boldsymbol{c}]$ **Population:** A chromosomes vector is provided as: $\boldsymbol{W} = [\boldsymbol{W}_{S_H}, \boldsymbol{W}_{V_H}, \boldsymbol{W}_{E_H}, \boldsymbol{W}_{I_H}, \boldsymbol{W}_{R_H}, \boldsymbol{W}_{A_N}, \boldsymbol{W}_{S_N}, \boldsymbol{W}_{E_N}, \boldsymbol{W}_{I_N}, \boldsymbol{W}_{A_W}, \boldsymbol{W}_{S_W}, \boldsymbol{W}_{E_W}, \boldsymbol{W}_{I_W}]$, for $\boldsymbol{W}_{S_H} = [\boldsymbol{k}_{S_H}, \boldsymbol{\omega}_{S_H}, \boldsymbol{c}_{S_H}]$, $\boldsymbol{W}_{V_H} = [\boldsymbol{k}_{V_H}, \boldsymbol{\omega}_{V_H}, \boldsymbol{c}_{V_H}]$, $\boldsymbol{W}_{E_H} = [\boldsymbol{k}_{E_H}, \boldsymbol{\omega}_{E_H}, \boldsymbol{c}_{E_H}]$, $\boldsymbol{W}_{I_H} = [\boldsymbol{k}_{I_H}, \boldsymbol{\omega}_{I_H}, \boldsymbol{c}_{I_H}]$, $\boldsymbol{W}_{R_H} = [\boldsymbol{k}_{R_H}, \boldsymbol{\omega}_{R_H}, \boldsymbol{c}_{R_H}]$, $\boldsymbol{W}_{A_N} = [\boldsymbol{k}_{A_N}, \boldsymbol{\omega}_{A_N}, \boldsymbol{c}_{A_N}]$, $\boldsymbol{W}_{S_N} = [\boldsymbol{k}_{S_N}, \boldsymbol{\omega}_{S_N}, \boldsymbol{a}_{S_N}]$, $\boldsymbol{W}_{E_N} = [\boldsymbol{k}_{E_N}, \boldsymbol{\omega}_{E_N}, \boldsymbol{c}_{E_N}]$, $\boldsymbol{W}_{I_N} = [\boldsymbol{k}_{I_N}, \boldsymbol{\omega}_{I_N}, \boldsymbol{c}_{I_N}]$, $\boldsymbol{W}_{A_W} = [\boldsymbol{k}_{A_W}, \boldsymbol{\omega}_{A_W}, \boldsymbol{c}_{A_W}]$, $\boldsymbol{W}_{S_W} = [\boldsymbol{k}_{S_W}, \boldsymbol{\omega}_{S_W}, \boldsymbol{c}_{S_W}]$, $\boldsymbol{W}_{E_W} = [\boldsymbol{k}_{E_W}, \boldsymbol{\omega}_{E_W}, \boldsymbol{c}_{E_W}]$ and $\boldsymbol{W}_{I_W} = [\boldsymbol{k}_{I_W}, \boldsymbol{\omega}_{I_W}, \boldsymbol{c}_{I_W}]$. **Outputs:** Global weight vectors are $\boldsymbol{W}_{\textbf{B-GA}}$ **Initialization:** For chromosomes selection, use $\boldsymbol{W}_{\textbf{B-GA}}$ **Fit Valuation:** Adjust the fitness (*e*) in population using Eqs 4-18 • **Stopping standards:** [Tol-Con=Tol-Fun=10^{-21}], [Stall-Limit=150], [Generations = 110], [e = 10^{-22}] & [Pop-Size=240]. Move to **storage** **Storage:** $\boldsymbol{W}_{\textbf{B-GA}}$, iterations, time, *e* and count of function. **End of GA**
ASA **Inputs:** $\boldsymbol{W}_{\textbf{B-GA}}$. **Output:** $\boldsymbol{W}_{\textbf{GA-ASA}}$ represents the GA-ASA best performances. **Initialize:** $\boldsymbol{W}_{\textbf{B-GA}}$, assignments, iterations, and other perks. **Stopping merits:** [e = 10^{-21}], [Tol-Con = 10^{-21}], [Iterations = 930], [Tol-X = Tol-Fun= 10^{-18}] and [Max-Fun-Evals= 247000]. **Fit Valuation:** Calculate $\boldsymbol{e}$ and $\boldsymbol{W}$ for Eqs 4-18. **Amendments:** Regulate 'fmincon' for ASA **Accumulate:** Transform *e*, $\boldsymbol{W}_{\textbf{GA-ASA}}$, time, function counts and iterations for ASA. **ASA End**

C. PERFORMANCE MEASURES

In this section, the statistical operator characteristics relying on "Theil's inequality coefficient (TIC)", "Variance account for (VAF)", "Mean absolute deviation (MAD)", and "Semi interquartile range (S.I.R)" are theoretically described in order to solve dengue mathematical model. (19)–(21), as shown at the bottom of pages 10 and 11, respectively.

$$\begin{cases} \text{S.I Range} = 0.5 \times (q_3 - q_1), \\ q_1 = 1^{st} \text{ quartile } \& \ q_3 = 3^{rd} \text{quartile}, \end{cases} \tag{22}$$

r shows the grid point, while $\hat{S}_H$, $\hat{V}_H$, $\hat{E}_H$, $\hat{I}_H$, $\hat{R}_H$, $\hat{A}_N$, $\hat{S}_N$, $\hat{E}_N$, $\hat{I}_N$, $\hat{A}_W$, $\hat{S}_W$ *and* $\hat{I}_W$ are the approximate outcomes.

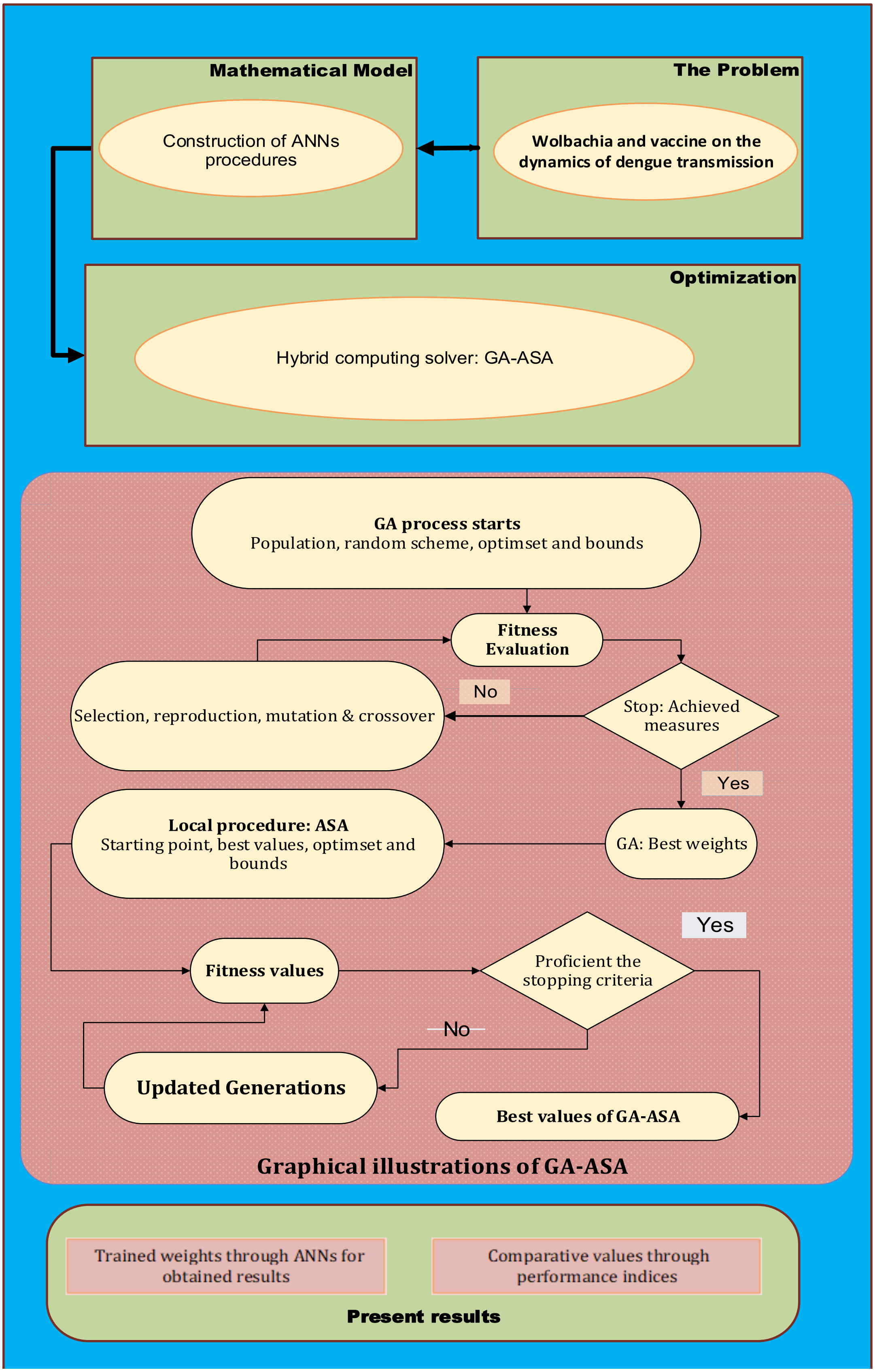

FIGURE 1. Structures of the existing approach to solve the mathematical dengue model.

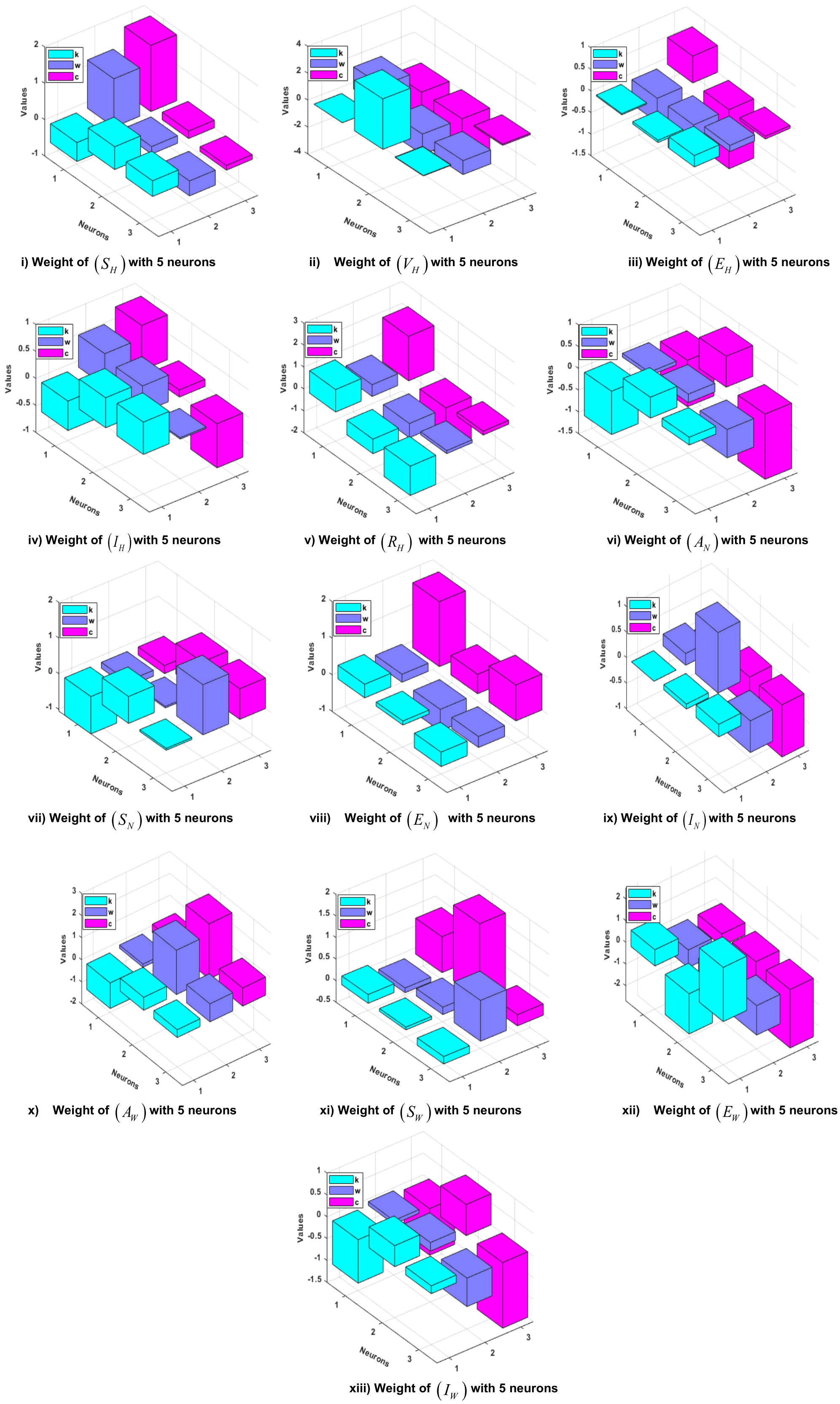

FIGURE 2. Trained weight of dengue model with best fitness.

IV. SIMULATIONS AND RESULTS

This section contains thorough reviews of the acquired findings for the dengue treatment in the presence of Wolbachia and non-Wolbachia (1). Equation (1) comprises the 3 cases of dengue reduction. (i) Vaccination (ii) Wolbachia treatment and (iii) Vaccination and Wolbachia combine. The Genetic Algorithm and active set algorithm is adopted for 0-1 inputs along 0.1 step size of the dengue mathematical model in equation (1). The findings of the Adams comparison show that the dengue modeling approach is valid. Moreover, statistical findings are provided to ensure that the planned procedure is precise and accurate.

$$\begin{aligned} S'_H(t) &= 0.0005852 - (1.3298)S_H(t) + 0.1V_H(t),\\ I_1 &= 0.1,\\ V'_H(t) &= 0.2S_H(t) - 0.4144V_H(t) - 0.1151V_H(t), \end{aligned}$$

$$\left\{\begin{aligned} &\begin{bmatrix} \mathrm{VAF}_{S_H}, \mathrm{VAF}_{V_H}, \mathrm{VAF}_{E_H}, \mathrm{VAF}_{I_H},\\ \mathrm{VAF}_{R_H}, \mathrm{VAF}_{A_N}, \mathrm{VAF}_{S_N}, \mathrm{VAF}_{E_N},\\ \mathrm{VAF}_{I_N}, \mathrm{VAF}_{A_W}, \mathrm{VAF}_{S_W}, \mathrm{VAF}_{E_W},\\ \mathrm{VAF}_{I_W} \end{bmatrix} = \begin{bmatrix} \left(1-\frac{\mathrm{var}\left((S_H)_r-(\hat{S}_H)_r\right)}{\mathrm{var}((S_H)_r)}\right)\times 100,\\ \left(1-\frac{\mathrm{var}\left((V_H)_r-(\hat{V}_H)_r\right)}{\mathrm{var}((V_H)_r)}\right)\times 100,\\ \left(1-\frac{\mathrm{var}\left((E_H)_r-(\hat{E}_H)_r\right)}{\mathrm{var}((E_H)_r)}\right)\times 100,\\ \left(1-\frac{\mathrm{var}\left((I_H)_r-(\hat{I}_H)_r\right)}{\mathrm{var}((I_H)_r)}\right)\times 100,\\ \left(1-\frac{\mathrm{var}\left((R_H)_r-(\hat{R}_H)_r\right)}{\mathrm{var}((R_H)_r)}\right)\times 100,\\ \left(1-\frac{\mathrm{var}\left((A_N)_r-(\hat{A}_N)_r\right)}{\mathrm{var}((A_N)_r)}\right)\times 100,\\ \left(1-\frac{\mathrm{var}\left((S_N)_r-(\hat{S}_N)_r\right)}{\mathrm{var}((S_N)_r)}\right)\times 100,\\ \left(1-\frac{\mathrm{var}\left((E_N)_r-(\hat{E}_N)_r\right)}{\mathrm{var}((E_N)_r)}\right)\times 100,\\ \left(1-\frac{\mathrm{var}\left((I_N)_r-(\hat{I}_N)_r\right)}{\mathrm{var}((I_N)_r)}\right)\times 100,\\ \left(1-\frac{\mathrm{var}\left((A_W)_r-(\hat{A}_W)_r\right)}{\mathrm{var}((A_W)_r)}\right)\times 100,\\ \left(1-\frac{\mathrm{var}\left((S_W)_r-(\hat{S}_W)_r\right)}{\mathrm{var}((S_W)_r)}\right)\times 100,\\ \left(1-\frac{\mathrm{var}\left((E_W)_r-(\hat{E}_W)_r\right)}{\mathrm{var}((E_W)_r)}\right)\times 100,\\ \left(1-\frac{\mathrm{var}\left((I_W)_r-(\hat{I}_W)_r\right)}{\mathrm{var}((I_W)_r)}\right)\times 100 \end{bmatrix}\\ &\begin{bmatrix} \mathrm{VAF}_{S_H}, \mathrm{VAF}_{V_H}, \mathrm{VAF}_{E_H}, \mathrm{VAF}_{I_H},\\ \mathrm{VAF}_{R_H}, \mathrm{VAF}_{A_N}, \mathrm{VAF}_{S_N}, \mathrm{VAF}_{E_N},\\ \mathrm{VAF}_{I_N}, \mathrm{VAF}_{A_W}, \mathrm{VAF}_{S_W}, \mathrm{VAF}_{E_W},\\ \mathrm{VAF}_{I_W} \end{bmatrix} = \left[\begin{vmatrix} 100-\mathrm{VAF}_{S_H}, 100-\mathrm{VAF}_{V_H},\\ 100-\mathrm{VAF}_{E_H}, 100-\mathrm{VAF}_{I_H},\\ 100-\mathrm{VAF}_{R_H}, 100-\mathrm{VAF}_{A_N},\\ 100-\mathrm{VAF}_{S_N}, 100-\mathrm{VAF}_{E_N},\\ 100-\mathrm{VAF}_{I_N}, 100-\mathrm{VAF}_{A_W},\\ 100-\mathrm{VAF}_{S_W}, 100-\mathrm{VAF}_{E_W},\\ 100-\mathrm{VAF}_{I_W} \end{vmatrix}\right]. \end{aligned}\right. \tag{19}$$

$$\begin{bmatrix} \mathrm{MAD}_{S_H}, \mathrm{MAD}_{V_H}, \mathrm{MAD}_{E_H},\\ \mathrm{MAD}_{I_H}, \mathrm{MAD}_{R_H}, \mathrm{MAD}_{A_N},\\ \mathrm{MAD}_{S_N}, \mathrm{MAD}_{E_N}, \mathrm{MAD}_{I_N},\\ \mathrm{MAD}_{A_W}, \mathrm{MAD}_{S_W}, \mathrm{MAD}_{E_W},\\ \mathrm{MAD}_{I_W} \end{bmatrix} = \begin{bmatrix} \sum_{r=1}^{n}\left|(S_H)_r-(\hat{S}_H)_r\right|, \sum_{r=1}^{n}\left|(V_H)_r-(\hat{V}_H)_r\right|,\\ \sum_{r=1}^{n}\left|(E_H)_r-(\hat{E}_H)_r\right|, \sum_{r=1}^{n}\left|(I_H)_r-(\hat{I}_H)_r\right|,\\ \sum_{r=1}^{n}\left|(R_H)_r-(\hat{R}_H)_r\right|, \sum_{r=1}^{n}\left|(A_N)_r-(\hat{A}_N)_r\right|,\\ \sum_{r=1}^{n}\left|(S_N)_r-(\hat{S}_N)_r\right|, \sum_{r=1}^{n}\left|(E_N)_r-(\hat{E}_N)_r\right|,\\ \sum_{r=1}^{n}\left|(I_N)_r-(\hat{I}_N)_r\right|, \sum_{r=1}^{n}(A_W)_r-(\hat{A}_W)_r,\\ \sum_{r=1}^{n}\left|(S_W)_r-(\hat{S}_W)_r\right|, \sum_{r=1}^{n}\left|(E_W)_r-(\hat{E}_W)_r\right|,\\ \sum_{r=1}^{n}\left|(I_W)_r-(\hat{I}_W)_r\right| \end{bmatrix}, \tag{20}$$

$$
\begin{aligned}
I_2 &= 0.1,\\
E'_H(t) &= 1.1147S_H(t) + 0.4144V_H(t) - 0.18204E_H(t),\\
I_3 &= 0.1,\\
I'_H(t) &= 0.182E_H(t) - 0.25I_H(t) - 0.0151S_H(t),\\
I_4 &= 0.1,\\
R'_H(t) &= 0.25I_H(t) - 0.0151R_H(t),\\
I_5 &= 0.1,\\
A'_N(t) &= 0.0833\left(1 - \frac{(A_N(t) + A_W(t))}{2}\right)\\
&\quad - 1.3214A_N(t),\\
I_6 &= 0.1,\\
S'_N(t) &= 1.15A_N(t) - 4.7052I_H(t)S_N(t) - 0.07S_N(t),\\
I_7 &= 0.1,\\
E'_N(t) &= 4.70521I_H(t)S_N(t) - 0.1E_N(t) - 0.07E_N(t),\\
I_8 &= 0.1,\\
I'_N(t) &= 0.1E_N(t) - 0.07I_N(t),\\
I_9 &= 0.1,\\
A'_W(t) &= 0.00687\left(2 - (A_N(t) + A_W(t))\right) + 0.03A_W(t),\\
I_{10} &= 0.1,\\
S'_W(t) &= 0.045A_W(t) - S_W(t)\\
&\quad \times \left(2.0263 + 4.46886I_H(t)\right),\\
I_{11} &= 0.1,\\
E'_W(t) &= 4.4686I_H(t)S_W(t) - 0.182E_W(t)\\
&\quad - 0.071E_W(t),\\
I_{12} &= 0.1,\\
I'_W(t) &= 0.182E_W(t) - 0.077I_W(t),\\
I_{13} &= 0.1. \qquad (23)
\end{aligned}
$$

Using the above system, the fitness function may be written as (24), shown at the bottom of the next page.

The dengue mathematical system is solved utilizing the hybrid GA-ASA for 100 iterations with 120 parameters by optimizing the above fitness function. The proposed solutions of the dengue mathematical system are represented by the best weight vectors, which are as follows:

$$
\begin{aligned}
\hat{S}_H(t) &= \frac{0.7473}{1 + e^{-(-0.8078t - 0.5602)}} - \frac{-1.8513}{1 + e^{-(-.8105t - 1.5264)}}\\
&\quad - \frac{2.4967}{1 + e^{-(-1.33565t - 2.6888)}}, \qquad (25)\\
\hat{V}_H(t) &= \frac{0.2023}{1 + e^{-(-0.1105t - 0.8327)}} - \frac{0.0652}{1 + e^{-(0.1713t + 1.7523)}}\\
&\quad - \frac{-0.1710}{1 + e^{-(0.9462t + 0.2607)}}, \qquad (26)
\end{aligned}
$$

$$
\begin{bmatrix}
\mathrm{TIC}_{S_H}, \mathrm{TIC}_{V_H},\\
\mathrm{TIC}_{E_H}, \mathrm{TIC}_{I_H},\\
\mathrm{TIC}_{R_H}, \mathrm{TIC}_{A_N},\\
\mathrm{TIC}_{S_N}, \mathrm{TIC}_{E_N},\\
\mathrm{TIC}_{I_N}, \mathrm{TIC}_{A_W},\\
\mathrm{TIC}_{S_W}, \mathrm{TIC}_{E_W},\\
\mathrm{TIC}_{I_W}
\end{bmatrix}
=
\begin{bmatrix}
\frac{\sqrt{\frac{1}{n}\sum_{r=1}^{n}\left((S_H)_r-(\hat{S}_H)_r\right)^2}}{\left(\sqrt{\frac{1}{n}\sum_{r=1}^{n}(S_H)_r^2}+\sqrt{\frac{1}{n}\sum_{r=1}^{n}(\hat{S}_H)_r^2}\right)}, & \frac{\sqrt{\frac{1}{n}\sum_{r=1}^{n}\left((V_H)_r-(\hat{V}_H)_r\right)^2}}{\left(\sqrt{\frac{1}{n}\sum_{r=1}^{n}(V_H)_r^2}+\sqrt{\frac{1}{n}\sum_{r=1}^{n}(\hat{V}_H)_r^2}\right)},\\
\frac{\sqrt{\frac{1}{n}\sum_{r=1}^{n}\left((E_H)_r-(\hat{E}_H)_r\right)^2}}{\left(\sqrt{\frac{1}{n}\sum_{r=1}^{n}(E_H)_r^2}+\sqrt{\frac{1}{n}\sum_{r=1}^{n}(\hat{E}_H)_r^2}\right)}, & \frac{\sqrt{\frac{1}{n}\sum_{r=1}^{n}\left((I_H)_r-(\hat{I}_H)_r\right)^2}}{\left(\sqrt{\frac{1}{n}\sum_{r=1}^{n}(I_H)_r^2}+\sqrt{\frac{1}{n}\sum_{r=1}^{n}(\hat{I}_H)_r^2}\right)},\\
\frac{\sqrt{\frac{1}{n}\sum_{r=1}^{n}\left((R_H)_r-(\hat{R}_H)_r\right)^2}}{\left(\sqrt{\frac{1}{n}\sum_{r=1}^{n}(R_H)_r^2}+\sqrt{\frac{1}{n}\sum_{r=1}^{n}(\hat{R}_H)_r^2}\right)}, & \frac{\sqrt{\frac{1}{n}\sum_{r=1}^{n}\left((E_W)_r-(\hat{E}_W)_r\right)^2}}{\left(\sqrt{\frac{1}{n}\sum_{r=1}^{n}(E_W)_r^2}+\sqrt{\frac{1}{n}\sum_{r=1}^{n}(\hat{E}_W)_r^2}\right)},\\
\frac{\sqrt{\frac{1}{n}\sum_{r=1}^{n}\left((I_W)_r-(\hat{I}_W)_r\right)^2}}{\left(\sqrt{\frac{1}{n}\sum_{r=1}^{n}(I_W)_r^2}+\sqrt{\frac{1}{n}\sum_{r=1}^{n}(\hat{I}_W)_r^2}\right)}, & \frac{\sqrt{\frac{1}{n}\sum_{r=1}^{n}\left((A_N)_r-(\hat{A}_N)_r\right)^2}}{\left(\sqrt{\frac{1}{n}\sum_{r=1}^{n}(A_N)_r^2}+\sqrt{\frac{1}{n}\sum_{r=1}^{n}(\hat{A}_N)_r^2}\right)},\\
\frac{\sqrt{\frac{1}{n}\sum_{r=1}^{n}\left((S_N)_r-(\hat{S}_N)_r\right)^2}}{\left(\sqrt{\frac{1}{n}\sum_{r=1}^{n}(S_N)_r^2}+\sqrt{\frac{1}{n}\sum_{r=1}^{n}(\hat{S}_N)_r^2}\right)}, & \frac{\sqrt{\frac{1}{n}\sum_{r=1}^{n}\left((E_N)_r-(\hat{E}_N)_r\right)^2}}{\left(\sqrt{\frac{1}{n}\sum_{r=1}^{n}(E_N)_r^2}+\sqrt{\frac{1}{n}\sum_{r=1}^{n}(\hat{E}_N)_r^2}\right)},\\
\frac{\sqrt{\frac{1}{n}\sum_{r=1}^{n}\left((I_N)_r-(\hat{I}_N)_r\right)^2}}{\left(\sqrt{\frac{1}{n}\sum_{r=1}^{n}(I_N)_r^2}+\sqrt{\frac{1}{n}\sum_{r=1}^{n}(\hat{I}_N)_r^2}\right)}, & \frac{\sqrt{\frac{1}{n}\sum_{r=1}^{n}\left((A_W)_r-(\hat{A}_W)_r\right)^2}}{\left(\sqrt{\frac{1}{n}\sum_{r=1}^{n}(A_W)_r^2}+\sqrt{\frac{1}{n}\sum_{r=1}^{n}(\hat{A}_W)_r^2}\right)},\\
\frac{\sqrt{\frac{1}{n}\sum_{r=1}^{n}\left((S_W)_r-(\hat{S}_W)_r\right)^2}}{\left(\sqrt{\frac{1}{n}\sum_{r=1}^{n}(S_W)_r^2}+\sqrt{\frac{1}{n}\sum_{r=1}^{n}(\hat{S}_W)_r^2}\right)} &
\end{bmatrix}, \qquad (21)
$$

TABLE 3. Statistical form for the dengue model based (S_H) class.

t	(S_H)					
	Min	**Max**	**Med**	**Mean**	**S.I Range**	**ST.D**
0	9.0119E-07	3.0444E-05	7.8165E-06	1.0058E-05	5.5727E-06	8.9102E-06
0.05	3.7423E-07	2.5754E-05	4.2771E-06	7.1361E-06	3.5672E-06	7.8253E-06
0.1	5.9058E-07	2.6260E-05	3.7032E-06	7.5301E-06	3.5474E-06	7.5801E-06
0.15	1.9850E-07	3.1778E-05	9.5762E-06	1.0995E-05	4.6081E-06	8.0832E-06
0.2	1.3148E-06	3.7704E-05	1.5796E-05	1.5166E-05	5.0600E-06	8.7289E-06
0.25	2.0960E-06	4.2165E-05	1.8732E-05	1.8457E-05	5.9925E-06	9.5456E-06
0.3	1.6505E-06	4.4103E-05	1.8670E-05	2.0329E-05	6.9399E-06	1.0692E-05
0.35	5.4068E-07	4.3109E-05	1.9400E-05	2.0624E-05	8.8440E-06	1.2200E-05
0.4	4.6515E-07	4.3539E-05	1.9377E-05	2.0443E-05	8.8407E-06	1.2021E-05
0.45	1.1320E-06	4.2514E-05	2.0047E-05	1.9293E-05	7.6501E-06	1.1305E-05
0.5	1.4241E-06	3.8804E-05	1.7343E-05	1.6799E-05	8.0163E-06	1.0780E-05
0.55	6.0147E-07	3.2855E-05	1.3060E-05	1.3536E-05	6.6635E-06	9.7397E-06
0.6	9.0710E-09	2.8290E-05	8.0802E-06	1.0025E-05	4.3658E-06	8.0140E-06
0.65	1.2809E-07	2.0351E-05	6.1322E-06	6.9766E-06	4.1943E-06	5.9087E-06
0.7	7.0510E-07	1.3073E-05	5.7889E-06	5.9150E-06	3.1439E-06	3.8942E-06
0.75	8.9725E-08	1.4835E-05	4.4094E-06	6.3250E-06	3.4339E-06	4.9033E-06
0.8	1.2538E-06	1.7678E-05	7.7740E-06	8.4981E-06	4.9879E-06	5.6778E-06
0.85	3.1750E-07	2.8242E-05	9.9109E-06	9.7936E-06	4.2978E-06	6.6571E-06
0.9	8.9169E-07	3.3816E-05	8.4099E-06	9.3942E-06	3.7136E-06	7.1088E-06
0.95	2.2563E-07	3.2089E-05	5.0364E-06	6.8002E-06	2.3532E-06	6.6200E-06
1	1.3103E-07	2.0733E-05	1.6795E-06	3.1559E-06	1.5291E-06	4.4429E-06

$$
\begin{aligned}
e = \frac{1}{N} \times \sum_{i=1}^{N} \Bigg(& \left[\hat{S}'_H - 0.0000413N_H + (\tfrac{0.165\hat{I}_N}{N_H} - 0.2000413 - \tfrac{0.078\hat{I}_H}{N_H})\hat{S}_H(t) - 0.1\,\hat{V}_H\right]^2 \\
& + \left[\hat{V}'_H - 0.2\hat{S}_H + 0.462\left(\tfrac{0.165\hat{I}_N + 0.078\hat{I}_H}{N_H}\right)\hat{V}_H - 0.1000413\,\hat{V}_H\right]^2 + \\
& \left[\hat{E}'_H - \left(\tfrac{0.165\hat{I}_N + 0.078\hat{I}_H}{N_H}\right)\hat{S}_H - 0.462\left(\tfrac{0.165\hat{I}_N + 0.078\hat{I}_H}{N_H}\right)\hat{V}_H - 0.18204\hat{E}_H\right]^2 \\
& + \left[\hat{I}'_H - 0.182\hat{E}_H + 0.25\hat{I}_H - 0.0000413\hat{S}_H\right]^2 + \left[\hat{R}'_H - 0.25\hat{I}_H + 0.0000413\hat{R}_H\right]^2 \\
& + \left[\hat{A}'_N - \tfrac{1.25}{2(F_N + F_W)}F_N^2\left(1 - \tfrac{\left(\hat{A}_N + \hat{A}_W\right)}{K}\right) + 1.3214\hat{A}_N\right]^2 \\
& + \left[\hat{S}'_N - \tfrac{1.25\hat{A}_N}{2} - 0.525\tfrac{\hat{A}_N}{} + \tfrac{0.164682\hat{I}_H\hat{S}_N}{N_H} + 0.07\hat{S}_N\right]^2 \\
& + \left[\hat{E}'_N - \tfrac{0.164682\hat{I}_H\hat{S}_N}{N_H} + 0.1\hat{E}_N + 0.07\hat{E}_N\right]^2 + \left[\hat{I}'_N - 0.1\hat{E}_N + 0.07\hat{I}_{Nr}\right]^2 \\
& + \left[\hat{A}'_W - \tfrac{0.275F_W}{2K}\,(K - (A_N(t) + A_W(t))) - 0.03\hat{A}_{Wr}\right]^2 \\
& + \left[\hat{S}'_W - 0.045\hat{A}_W - \tfrac{\hat{S}_W}{N_H}\left(0.077 + 0.1564\hat{I}_H\right)\right]^2 \\
& + \left[\hat{E}'_W - \tfrac{0.1564\hat{I}_H\hat{S}_W}{N_H} + 0.182\hat{E}_W + 0.071\hat{E}_W\right]^2 + \left[\hat{I}'_W - 0.182\hat{E}_W + 0.077\hat{I}_{Wr}\right]^2 \Bigg) \\
+ \frac{1}{13} \Bigg[& \left((\hat{S}'_H)_0 - 0.1\right)^2 + \left((\hat{V}'_H)_0 - 0.1\right)^2 + \left((\hat{E}'_H)_0 - 0.1\right)^2 + \left((\hat{I}'_H)_0 - 0.1\right)^2 + \left((\hat{R}'_H)_0 - 0.1\right)^2 \\
& + \left((\hat{A}'_H)_0 - 0.1\right)^2 + \left((\hat{S}'_N)_0 - 0.1\right)^2 + \left((\hat{E}'_{NH})_0 - 0.1\right)^2 + \left((\hat{I}'_N)_0 - 0.1\right)^2 + \left((\hat{A}'_H)_0 - 0.1\right)^2 \\
& + \left((\hat{S}'_W)_0 - 0.1\right)^2 + \left((\hat{E}'_H)_0 - 0.1\right)^2 + \left((\hat{I}'_H)_0 - 0.1\right)^2 \Bigg]. \qquad (24)
\end{aligned}
$$

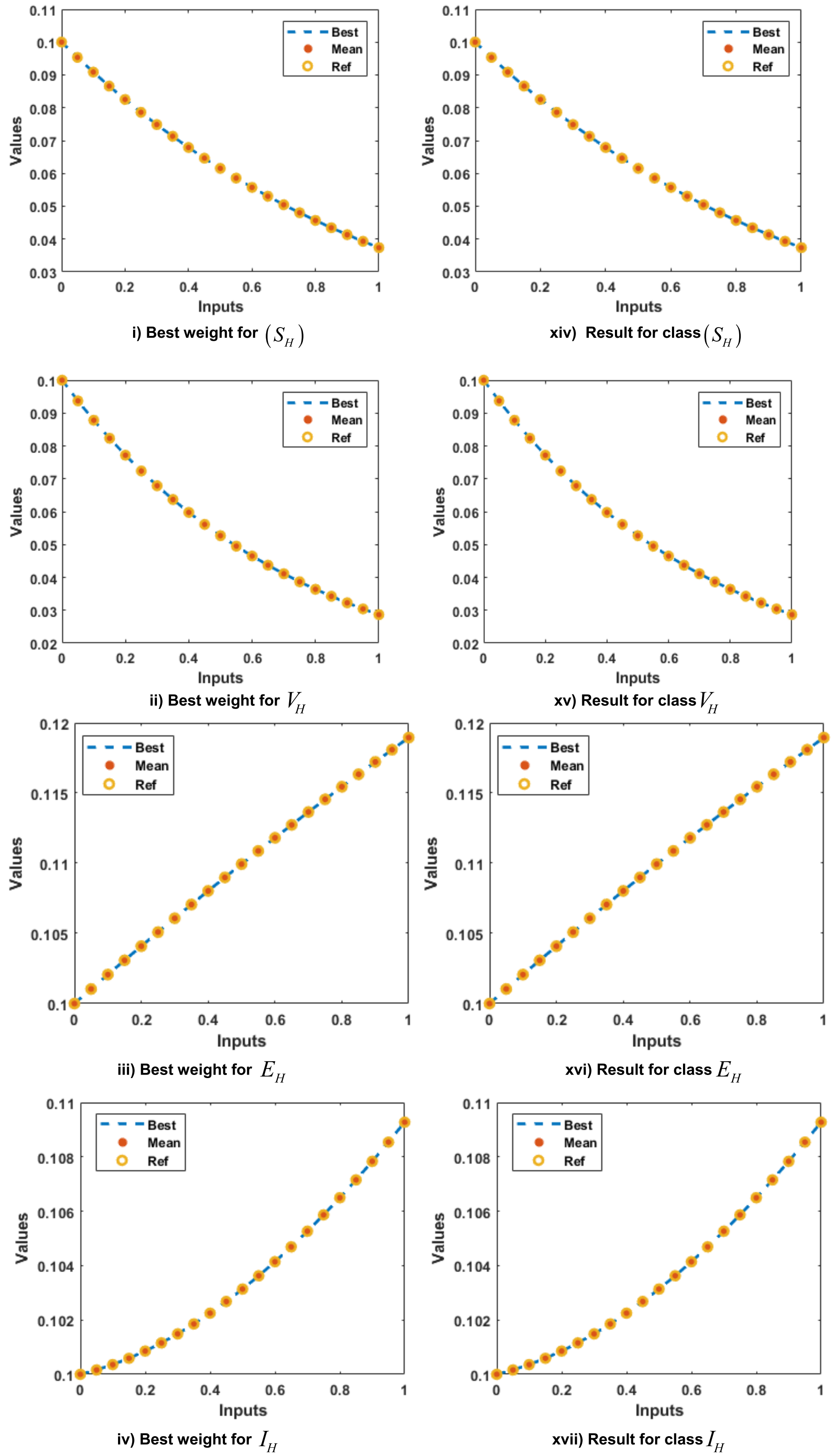

FIGURE 3. **The comparison of best, reference and mean solutions for the dengue system.**

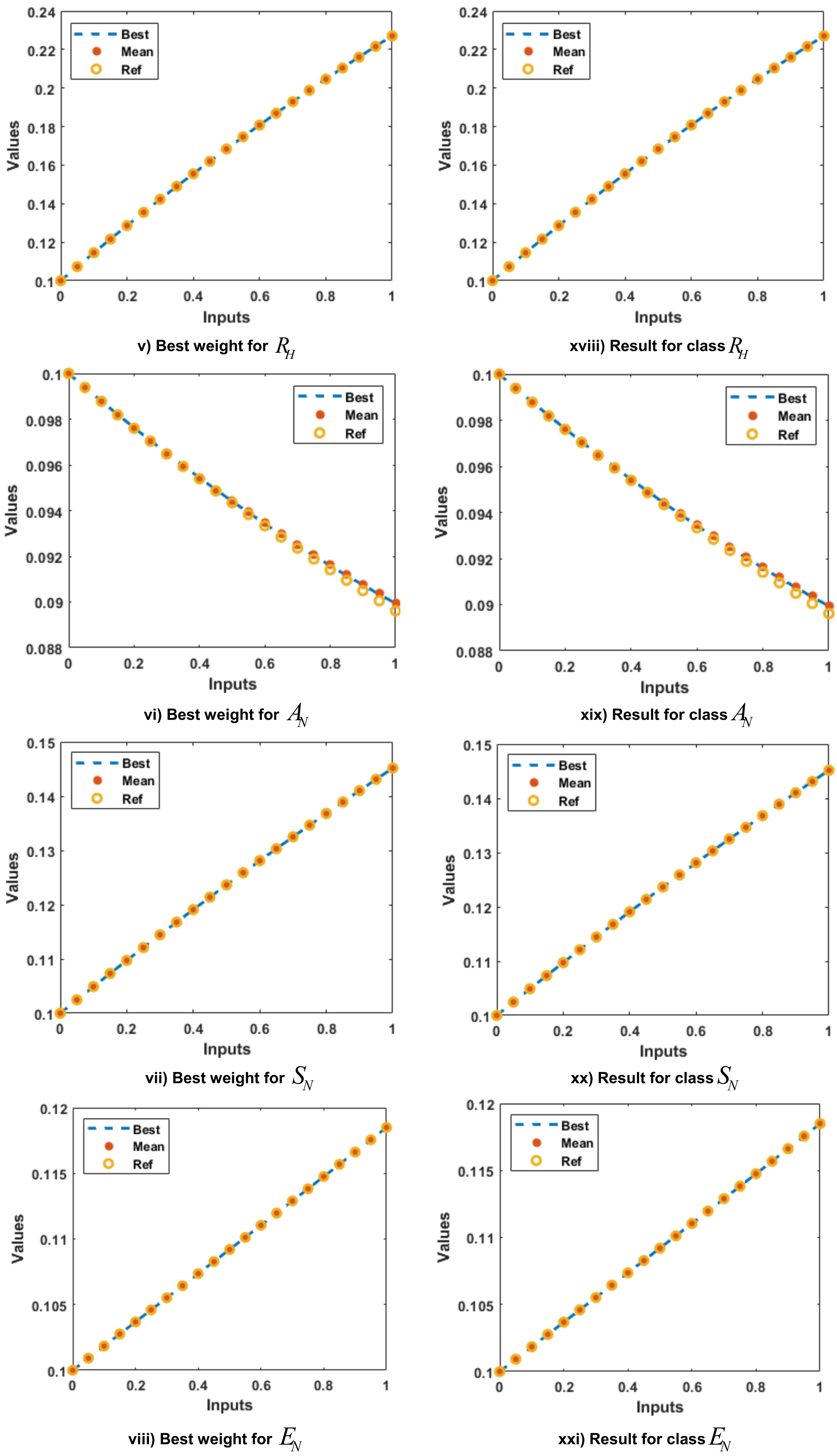

v) Best weight for R_H

xviii) Result for class R_H

vi) Best weight for A_N

xix) Result for class A_N

vii) Best weight for S_N

xx) Result for class S_N

viii) Best weight for E_N

xxi) Result for class E_N

FIGURE 3. ***(Continued.)*** **The comparison of best, reference and mean solutions for the dengue system.**

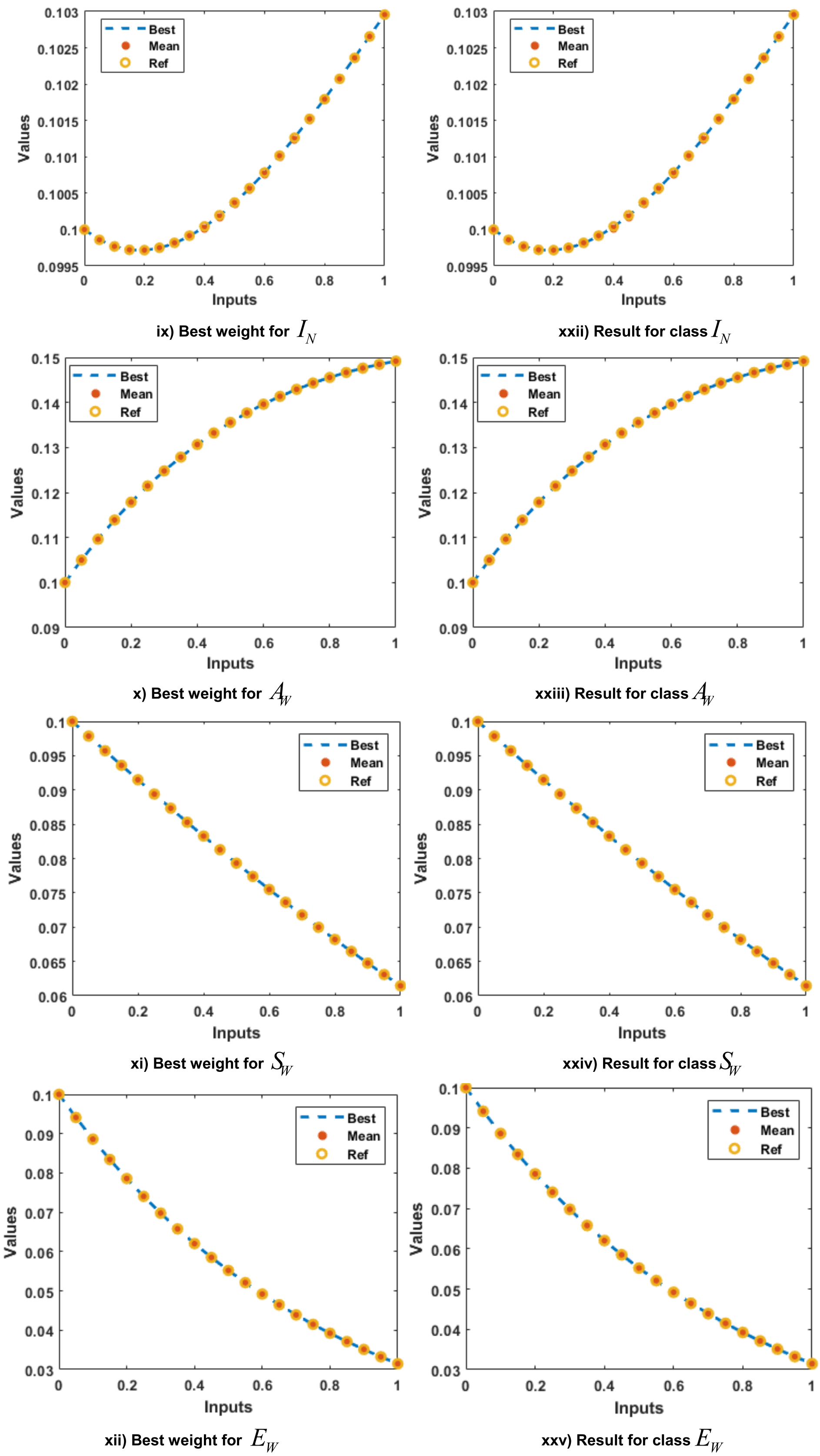

ix) Best weight for I_N

xxii) Result for class I_N

x) Best weight for A_W

xxiii) Result for class A_W

xi) Best weight for S_W

xxiv) Result for class S_W

xii) Best weight for E_W

xxv) Result for class E_W

FIGURE 3. ***(Continued.)*** **The comparison of best, reference and mean solutions for the dengue system.**

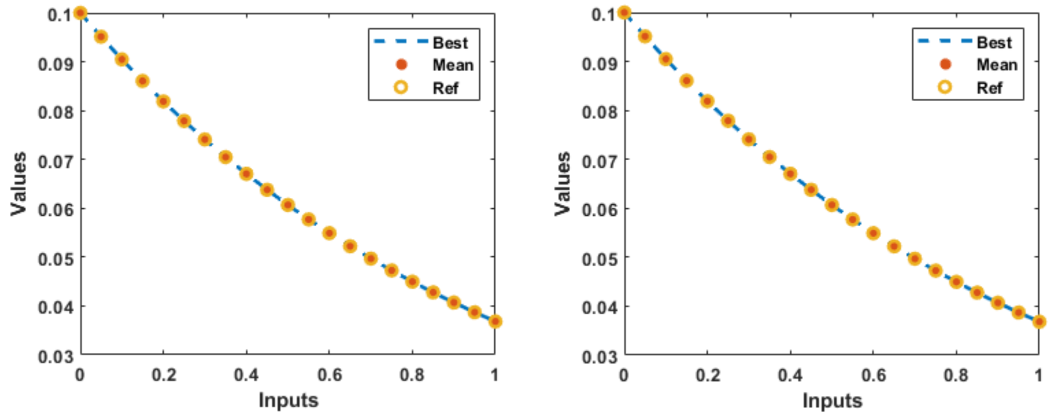

xiii) Best weight for I_W xxvi) Result for class I_W

FIGURE 3. ***(Continued.)*** **The comparison of best, reference and mean solutions for the dengue system.**

TABLE 4. **Statistical form for the dengue model based (V_H) and (E_H) classes.**

t	(V_H)			(E_H)		
	Min	**Mean**	**SIR**	**Min**	**Mean**	**SIR**
0	3.6422E-07	6.5115E-06	2.7337E-06	7.5419E-09	3.6699E-06	2.0173E-06
0.05	5.2119E-07	6.5544E-06	4.9721E-06	4.0348E-07	5.4235E-06	3.0752E-06
0.1	4.1417E-08	5.3032E-06	3.4655E-06	9.3905E-08	5.8395E-06	2.7715E-06
0.15	2.5081E-08	3.1696E-06	1.6652E-06	1.1956E-06	8.4596E-06	3.7464E-06
0.2	1.2513E-07	3.7049E-06	1.6638E-06	5.4210E-07	1.3313E-05	6.9568E-06
0.25	1.8019E-06	6.6436E-06	2.6579E-06	4.4302E-08	1.8309E-05	1.0745E-05
0.3	2.2371E-06	1.0330E-05	3.5366E-06	8.8951E-07	2.2846E-05	1.2980E-05
0.35	1.5874E-06	1.3436E-05	4.5109E-06	1.3166E-06	2.5320E-05	1.3583E-05
0.4	4.1607E-07	1.5636E-05	4.6203E-06	2.8165E-06	2.6679E-05	1.2005E-05
0.45	4.5545E-07	1.7393E-05	4.5637E-06	4.3227E-06	2.6236E-05	1.1362E-05
0.5	6.0411E-07	1.8274E-05	4.0531E-06	5.4209E-07	2.4372E-05	1.1389E-05
0.55	2.7215E-06	1.8480E-05	3.4664E-06	2.8862E-06	2.1930E-05	1.2365E-05
0.6	3.3306E-06	1.7784E-05	6.4698E-06	1.9315E-06	1.8005E-05	9.2645E-06
0.65	6.9005E-07	1.6294E-05	7.0020E-06	1.9474E-06	1.3781E-05	5.7768E-06
0.7	6.3459E-07	1.5131E-05	6.9748E-06	1.0868E-06	9.5022E-06	3.6048E-06
0.75	3.4524E-08	1.4662E-05	7.8556E-06	6.5266E-07	9.1659E-06	3.2564E-06
0.8	2.5847E-07	1.4968E-05	9.5660E-06	2.3698E-07	1.1440E-05	7.3359E-06
0.85	7.9934E-07	1.5434E-05	1.0342E-05	3.6194E-07	1.3411E-05	7.8354E-06
0.9	4.2685E-08	1.4725E-05	9.8697E-06	5.9012E-08	1.3918E-05	7.3681E-06
0.95	2.5231E-07	1.2342E-05	8.7474E-06	3.8457E-08	1.2114E-05	6.1957E-06
1	1.4343E-07	7.7854E-06	6.4931E-06	1.5980E-06	8.4306E-06	3.6624E-06

$$\hat{E}_H(t) = \frac{-1.1560}{1+e^{-(0.1434t+0.3753)}} - \frac{0.5852}{1+e^{-(2.0046t+2.4891)}} - \frac{0.3524}{1+e^{-(0.8160t+0.8222)}}, \tag{27}$$

$$\hat{I}_H(t) = \frac{0.0009178}{1+e^{-(0.2297t-0.1076)}} - \frac{0.0975}{1+e^{-(1.1845t-0.5986)}} - \frac{0.2455}{1+e^{-(-0.6195t-1.0212)}}, \tag{28}$$

$$\hat{R}_H(t) = \frac{0.3716}{1+e^{-(0.2188t+1.7740)}} - \frac{0.1099}{1+e^{-(-0.5871t+0.5293)}} - \frac{-0.3944}{1+e^{-(-0.2998+0.9808)}}, \tag{29}$$

$$\hat{A}_N(t) = \frac{-1.0474}{1+e^{-(-0.1646t-0.2226)}} - \frac{0.7539}{1+e^{-(0.0439t+0.8545)}} - \frac{0.0524}{1+e^{-(1.4054t+0.8575)}}, \tag{30}$$

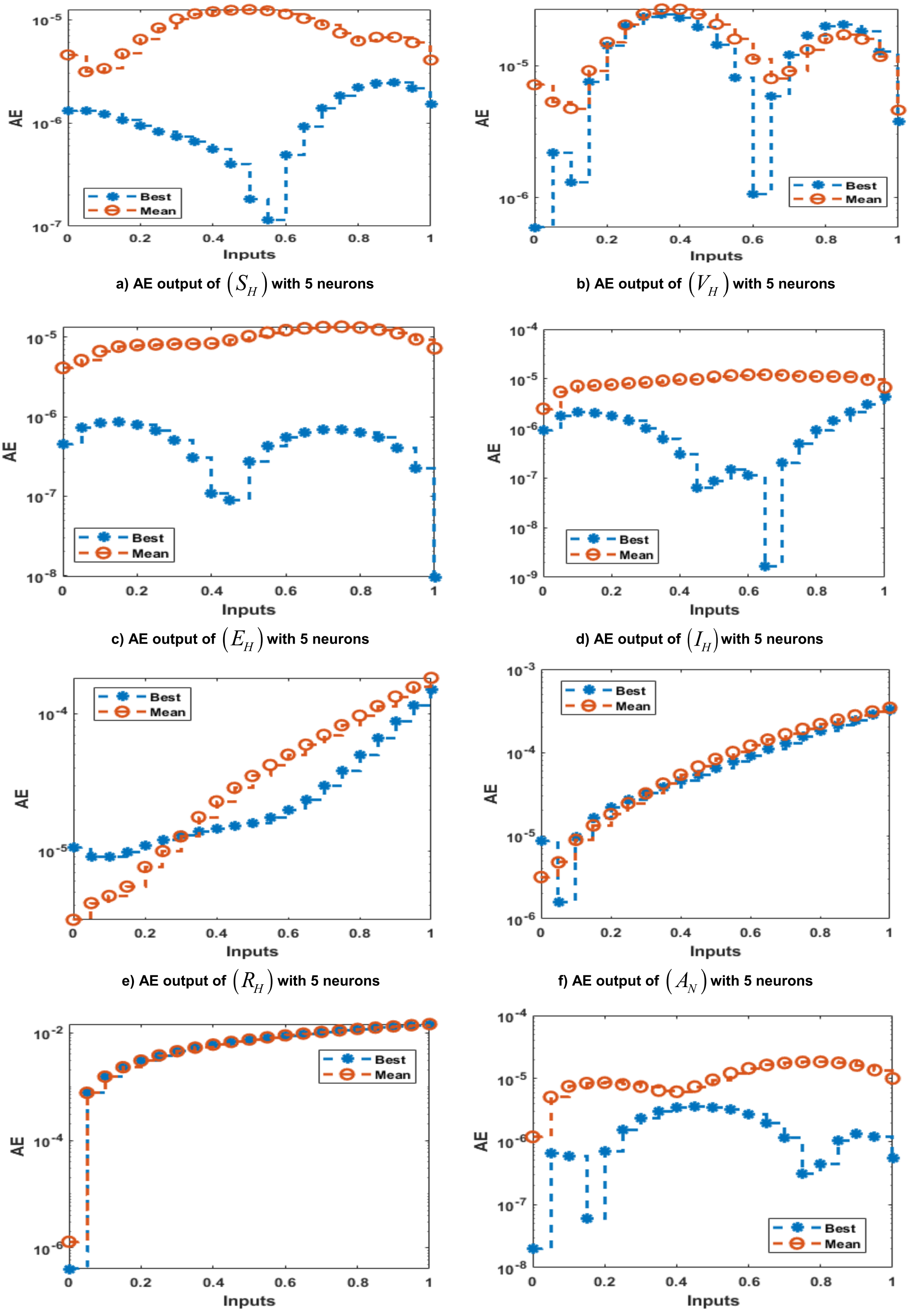

a) AE output of (S_H) with 5 neurons

b) AE output of (V_H) with 5 neurons

c) AE output of (E_H) with 5 neurons

d) AE output of (I_H) with 5 neurons

e) AE output of (R_H) with 5 neurons

f) AE output of (A_N) with 5 neurons

g) AE output of (S_N) with 5 neurons

h) AE output of (E_N) with 5 neurons

FIGURE 4. Relative observation of absolute errors for 5 number of neurons.

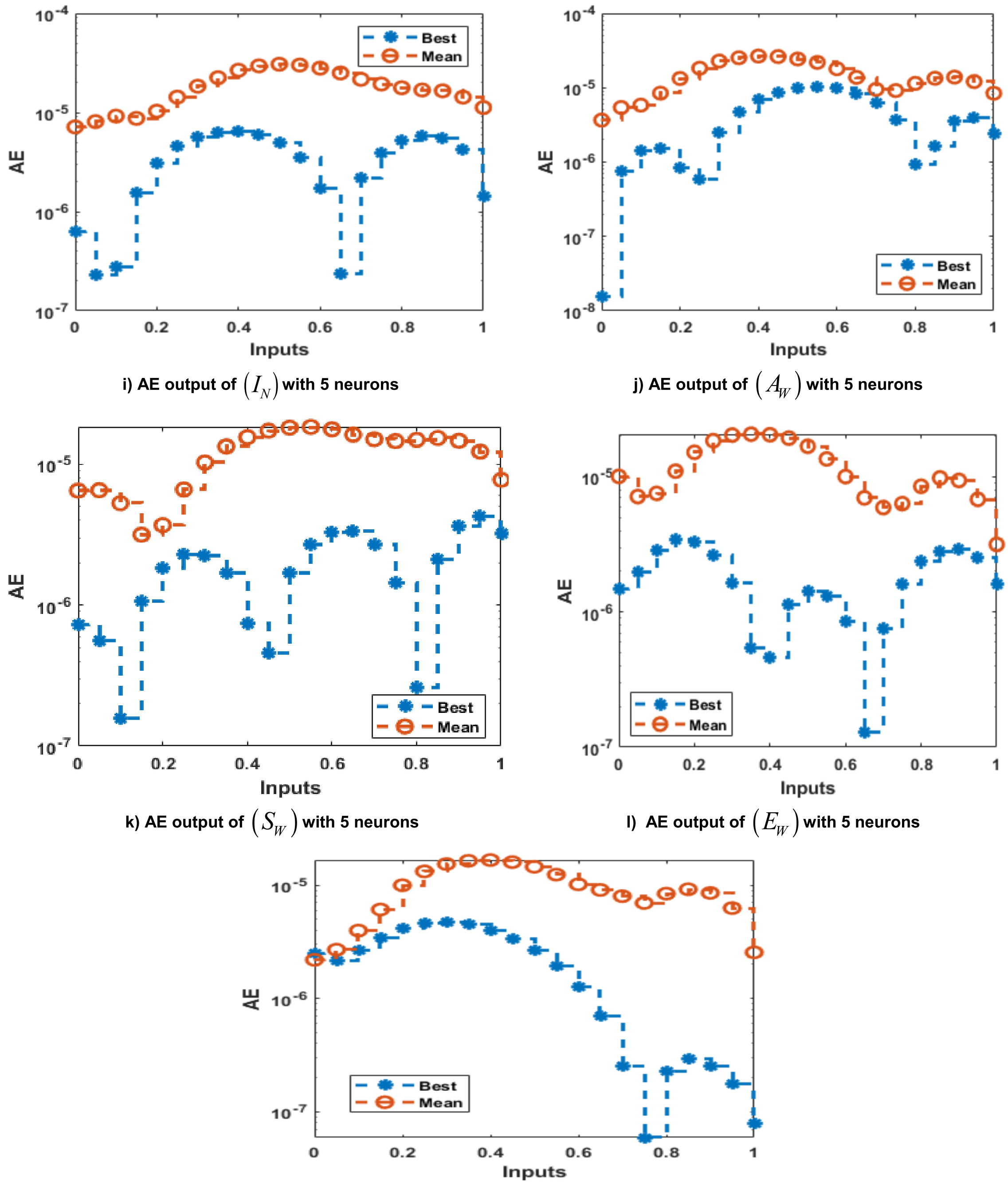

i) AE output of (I_N) with 5 neurons

j) AE output of (A_W) with 5 neurons

k) AE output of (S_W) with 5 neurons

l) AE output of (E_W) with 5 neurons

m) AE output of (I_W) with 5 neurons

FIGURE 4. ***(Continued.)*** **Relative observation of absolute errors for 5 number of neurons.**

$$\hat{S}_N(t) = \frac{-0.9953}{1+e^{-(0.0833t-1.0666)}} - \frac{0.4806}{1+e^{-(0.1958t+0.7104)}} - \frac{0.1787}{1+e^{-(-0.6518t-1.4993)}}, \tag{31}$$

$$\hat{E}_N(t) = \frac{1.0246}{1+e^{-(0.5340t+2.0261)}} - \frac{-0.6639}{1+e^{-(-0.6442t-1.9707)}} - \frac{-1.3326}{1+e^{-(-0.1368+0.1736)}}, \tag{32}$$

$$\hat{I}_N(t) = \frac{-0.5449}{1+e^{-(0.5943t+0.8333)}} - \frac{0.5565}{1+e^{-(0.4906t+0.1319)}} - \frac{0.5985}{1+e^{-(0.0263t-08180)}}, \tag{33}$$

$$\hat{A}_W(t) = \frac{-0.0265}{1+e^{-(-0.5592t+0.6220)}} - \frac{-0.0525}{1+e^{-(-0.9524t-1.3714)}} - \frac{0.2641}{1+e^{-(0.1429t-0.0633)}}, \tag{34}$$

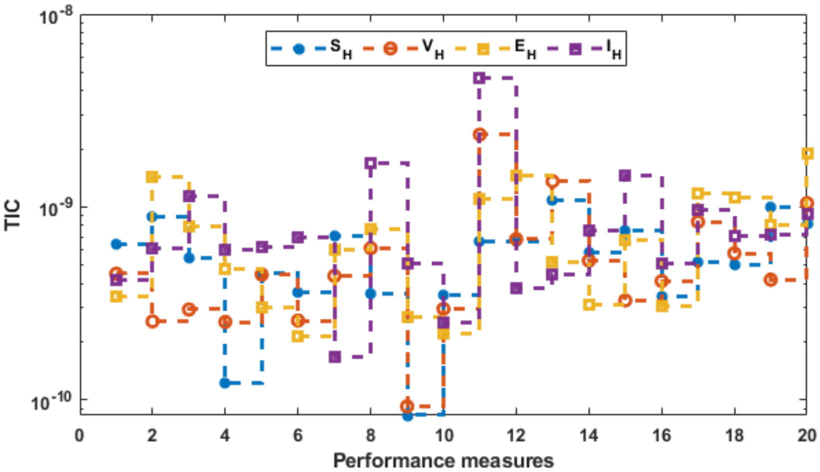

a) Convergence measurements for (S_H), (V_H), (E_H), and (I_H) on TIC in the y-axis, and independent dengue model trials in the x-axis.

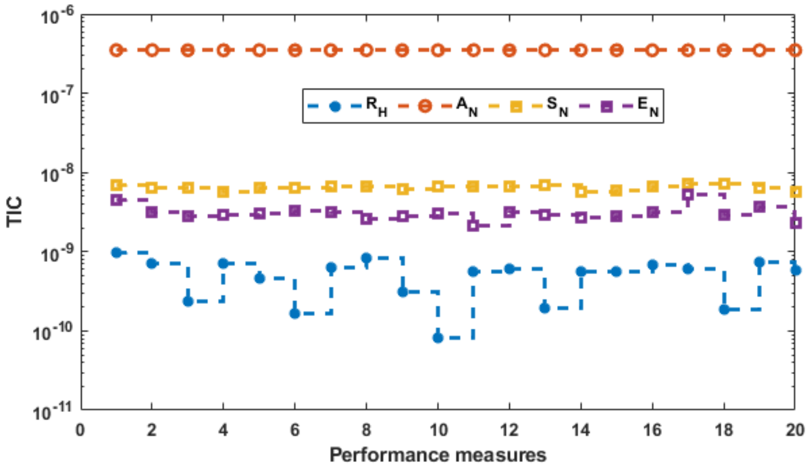

b) Convergence measurements for (R_H), (A_N), (S_N), and (E_N) on TIC in the y-axis, and independent dengue model trials in the x-axis.

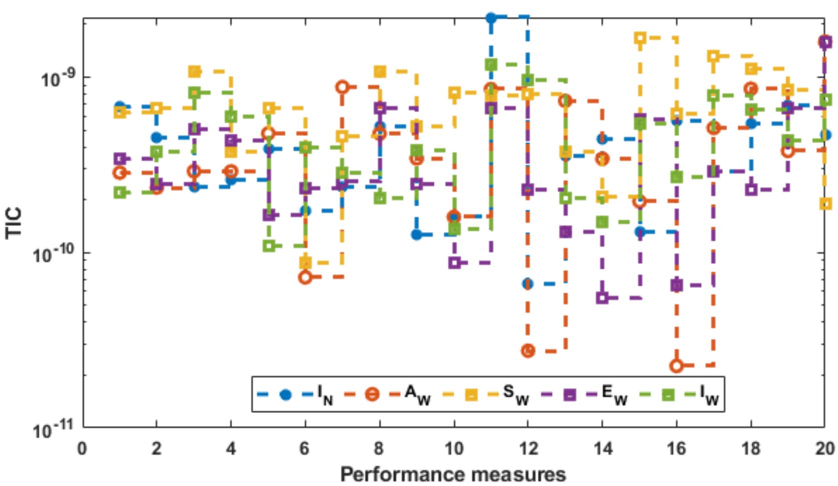

c) Convergence measures for (I_N), (A_W), (S_W), (E_W) and (I_W) on TIC in the y-axis, and independent dengue model trials in the x-axis.

FIGURE 5. Convergence schemes for the TIC values to solve the dengue nonlinear model.

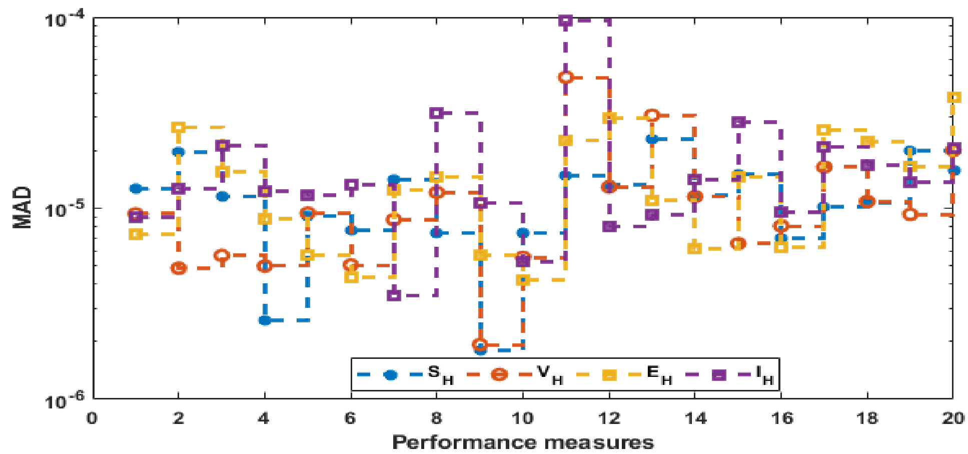

a) Convergence measurements for (S_H), (V_H), (E_H), and (I_H) on MAD in the y-axis, and independent dengue model trials in the x-axis.

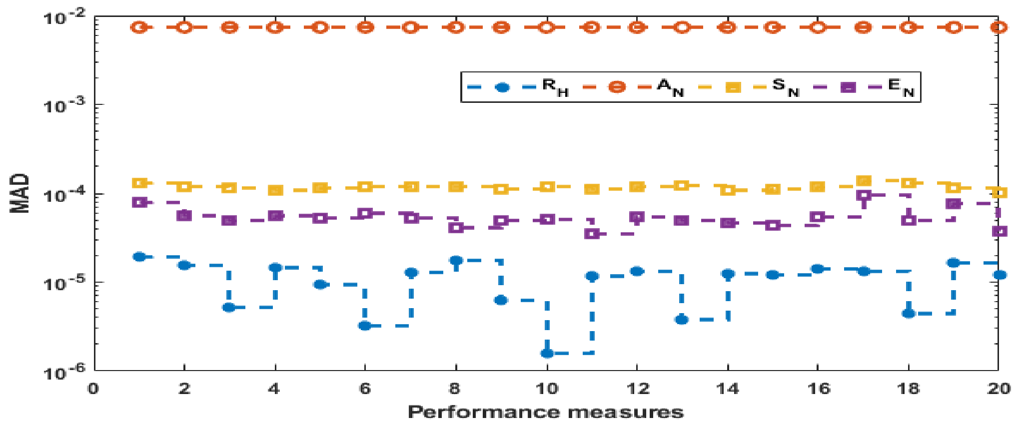

b) Convergence measures for (R_H), (A_N), (S_N), and (E_N) on MAD in the y-axis, and independent dengue model trials in the x-axis.

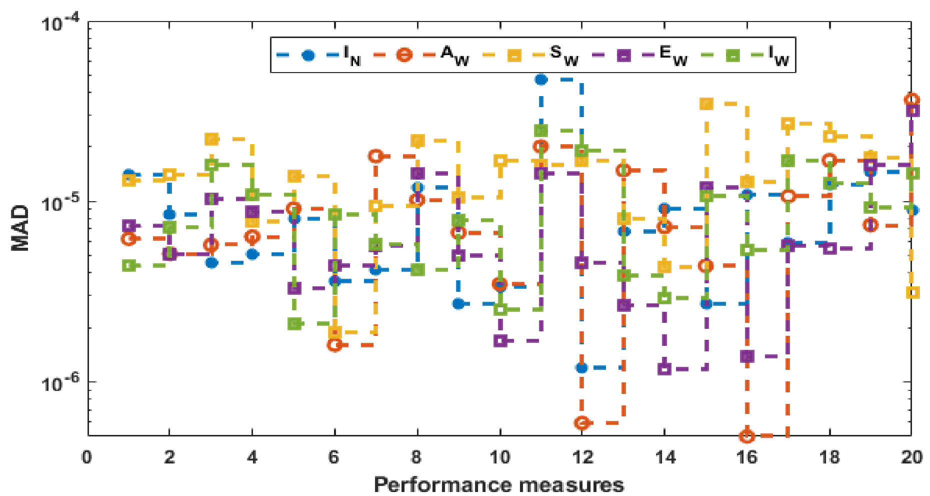

c) Convergence measures for (I_N), (A_W), (S_W), (E_W) and (I_W) on MAD in the y-axis, and independent dengue model trials in the x-axis.

FIGURE 6. Convergence schemes for the MAD values to solve the dengue nonlinear model.

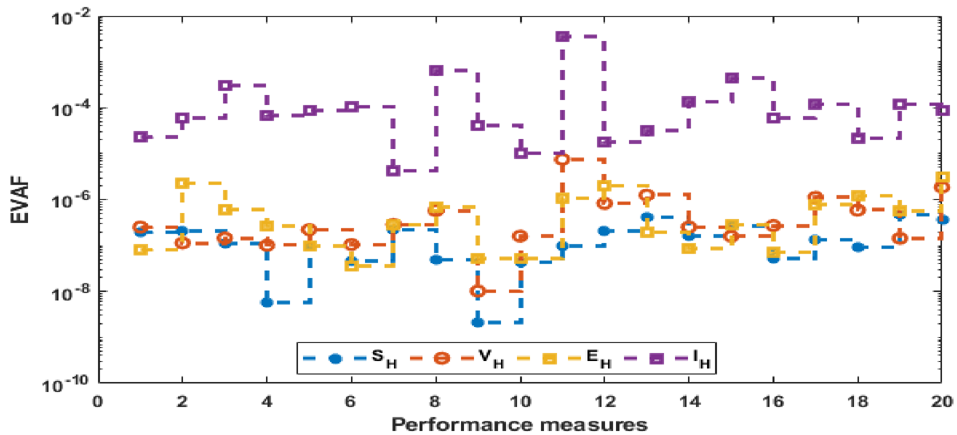

a) Convergence measures for (S_H), (V_H), (E_H), and (I_H) on EVAF in the y-axis, and independent dengue model trials in the x-axis.

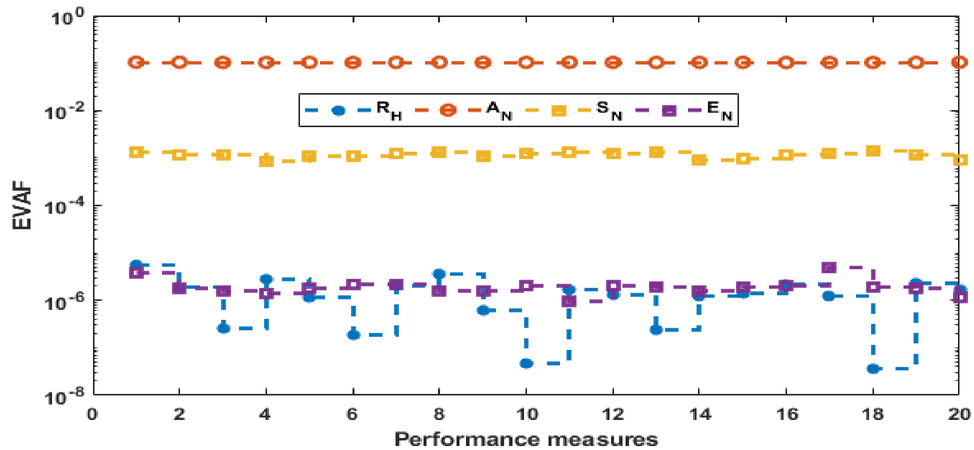

b) Convergence measures for (R_H), (A_N), (S_N), and (E_N) on EVAF in the y-axis, and independent dengue model trials in the x-axis.

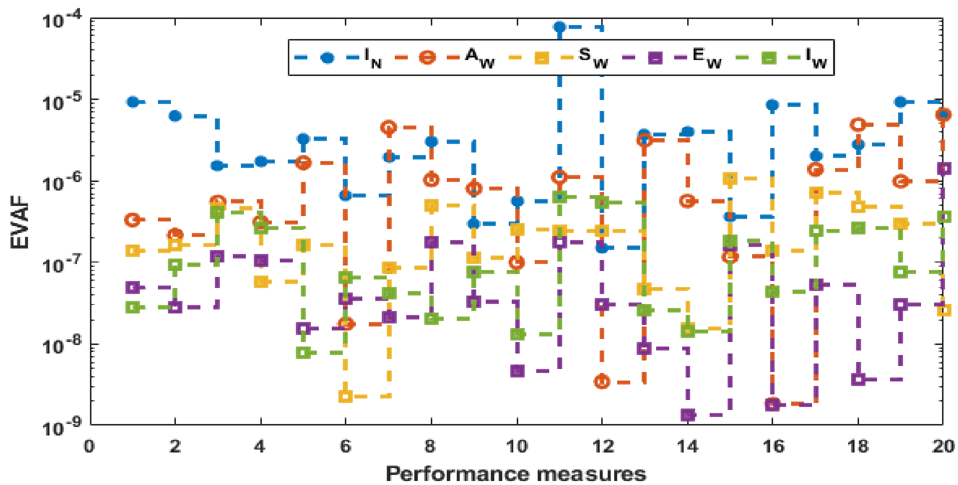

c) Convergence measures for (I_N), (A_W), (S_W), (E_W) and (I_W) on EVAF in the y-axis, and independent dengue model trials in the x-axis.

FIGURE 7. Convergence plans for the EVAF values to solve the dengue nonlinear model.

TABLE 5. Statistical form for the dengue model based (I_H) and (R_H) classes.

t	(I_H)			(R_H)		
	Min	Mean	SIR	Min	Mean	SIR
0	6.8759E-08	7.1580E-06	6.6030E-07	1.9753E-08	1.1876E-06	6.6030E-07
0.05	2.3127E-07	8.0927E-06	2.7552E-06	5.8774E-07	5.0776E-06	2.7552E-06
0.1	2.7678E-07	9.1988E-06	4.6141E-06	4.4038E-09	7.5132E-06	4.6141E-06
0.15	8.5945E-07	8.7245E-06	5.5475E-06	6.0788E-08	8.4415E-06	5.5475E-06
0.2	2.3589E-07	1.0316E-05	5.0755E-06	5.3117E-07	8.5977E-06	5.0755E-06
0.25	1.9916E-06	1.4301E-05	4.1884E-06	6.8261E-08	8.0375E-06	4.1884E-06
0.3	2.3096E-06	1.8415E-05	3.1132E-06	2.3372E-06	7.4379E-06	3.1132E-06
0.35	2.0664E-06	2.2480E-05	3.4069E-06	6.8024E-07	6.4427E-06	3.4069E-06
0.4	1.1085E-06	2.6726E-05	3.1850E-06	2.5349E-07	6.1583E-06	3.1850E-06
0.45	1.3300E-06	2.9531E-05	2.9512E-06	2.0032E-07	7.4419E-06	2.9512E-06
0.5	3.3303E-06	3.0699E-05	3.8385E-06	3.8055E-07	9.5303E-06	3.8385E-06
0.55	3.2109E-06	3.0116E-05	5.0687E-06	2.6708E-07	1.2142E-05	5.0687E-06
0.6	1.2149E-06	2.8046E-05	6.2759E-06	1.1715E-06	1.4489E-05	6.2759E-06
0.65	2.3925E-07	2.5034E-05	6.9703E-06	1.9542E-06	1.6355E-05	6.9703E-06
0.7	1.0334E-06	2.1624E-05	7.8247E-06	1.1441E-06	1.7626E-05	7.8247E-06
0.75	1.8793E-06	1.9380E-05	8.3431E-06	3.1358E-07	1.8308E-05	8.3431E-06
0.8	1.0064E-06	1.7776E-05	8.2485E-06	4.4313E-07	1.8420E-05	8.2485E-06
0.85	1.9363E-07	1.6869E-05	8.3080E-06	1.0235E-06	1.7732E-05	8.3080E-06
0.9	4.5808E-07	1.6550E-05	7.7312E-06	1.3135E-06	1.6144E-05	7.7312E-06
0.95	1.0644E-06	1.4301E-05	6.4529E-06	9.5472E-07	1.3594E-05	6.4529E-06
1	1.4327E-06	1.1225E-05	4.7152E-06	5.4109E-07	1.0031E-05	4.7152E-06

TABLE 6. Statistical form for the dengue model based (A_N) and (S_N) classes.

t	(A_N)			(S_N)		
	Min	Mean	SIR	Min	Mean	SIR
0	3.9986E-08	1.3070E-06	6.3971E-07	1.1826E-07	3.1741E-06	1.3048E-06
0.05	7.4790E-04	7.6505E-04	3.0964E-06	6.0299E-07	4.7772E-06	2.4540E-06
0.1	1.5031E-03	1.5264E-03	5.8109E-06	2.7733E-06	8.8789E-06	3.3144E-06
0.15	2.2581E-03	2.2842E-03	7.5700E-06	6.0040E-06	1.3280E-05	3.3605E-06
0.2	3.0119E-03	3.0381E-03	7.9224E-06	2.6973E-08	1.8125E-05	3.5124E-06
0.25	3.7638E-03	3.7879E-03	8.0957E-06	7.1703E-06	2.4493E-05	3.2025E-06
0.3	4.5129E-03	4.5334E-03	5.6376E-06	9.5425E-07	3.2112E-05	3.3380E-06
0.35	5.2586E-03	5.2744E-03	3.8691E-06	1.1961E-05	4.2074E-05	2.7576E-06
0.4	5.9958E-03	6.0107E-03	2.4351E-06	2.5950E-05	5.3826E-05	2.6889E-06
0.45	6.7277E-03	6.7422E-03	5.2662E-06	4.2913E-05	6.7482E-05	3.7117E-06
0.5	7.4517E-03	7.4688E-03	8.4429E-06	6.2751E-05	8.3120E-05	4.8389E-06
0.55	8.1712E-03	8.1903E-03	1.0613E-05	7.6837E-05	1.0078E-04	6.5836E-06
0.6	8.8845E-03	8.9067E-03	1.2218E-05	9.1791E-05	1.2047E-04	6.8966E-06
0.65	9.5916E-03	9.6180E-03	1.4398E-05	1.0945E-04	1.4216E-04	6.6988E-06
0.7	1.0294E-02	1.0324E-02	1.5872E-05	1.3003E-04	1.6580E-04	7.6023E-06
0.75	1.0993E-02	1.1025E-02	1.8000E-05	1.5374E-04	1.9131E-04	8.3460E-06
0.8	1.1688E-02	1.1720E-02	1.8524E-05	1.8073E-04	2.1859E-04	9.0482E-06
0.85	1.2380E-02	1.2411E-02	1.8087E-05	2.1044E-04	2.4752E-04	9.4689E-06
0.9	1.3068E-02	1.3096E-02	1.5800E-05	2.4367E-04	2.7797E-04	9.0129E-06
0.95	1.3753E-02	1.3776E-02	1.2377E-05	2.8101E-04	3.0979E-04	7.5381E-06
1	1.4435E-02	1.4451E-02	7.3635E-06	3.2264E-04	3.4282E-04	4.6908E-06

TABLE 7. Statistical form for the dengue model based (E_N) and (I_N) classes.

t	(E_N)			(I_N)		
	Min	Mean	SIR	Min	Mean	SIR
0	6.7817E-08	3.1481E-06	1.5148E-06	3.7997E-08	2.4965E-06	5.6616E-07
0.05	6.1056E-07	4.1646E-06	7.9355E-07	8.2454E-08	5.4743E-06	1.9614E-06
0.1	3.8718E-07	4.6992E-06	1.6388E-06	3.1200E-07	7.1752E-06	2.0987E-06
0.15	1.7872E-07	5.4966E-06	2.3462E-06	5.0197E-08	7.4165E-06	3.5179E-06
0.2	2.4110E-07	7.6291E-06	2.2365E-06	6.0621E-07	7.6521E-06	4.4114E-06
0.25	9.9928E-07	9.9748E-06	1.8943E-06	3.7268E-07	8.1770E-06	3.3622E-06
0.3	1.1497E-06	1.2751E-05	3.1555E-06	3.0067E-07	8.5030E-06	4.6976E-06
0.35	4.0627E-06	1.7631E-05	3.7362E-06	4.0227E-07	9.1942E-06	5.6627E-06
0.4	6.9358E-06	2.2972E-05	4.9581E-06	3.0425E-07	9.7818E-06	6.2956E-06
0.45	1.1060E-05	2.8798E-05	7.3598E-06	6.3480E-08	9.7856E-06	6.2793E-06
0.5	1.6060E-05	3.5195E-05	7.8271E-06	6.0136E-08	1.0983E-05	6.6834E-06
0.55	1.7465E-05	4.2308E-05	7.8929E-06	1.4528E-07	1.1729E-05	7.0932E-06
0.6	1.9852E-05	5.0334E-05	8.3368E-06	1.1485E-07	1.2077E-05	6.2800E-06
0.65	2.3729E-05	5.9512E-05	8.0676E-06	1.6628E-09	1.2087E-05	5.3430E-06
0.7	2.9676E-05	7.0121E-05	6.8826E-06	2.0423E-07	1.1765E-05	4.9978E-06
0.75	3.8339E-05	8.2467E-05	6.8887E-06	4.9059E-09	1.1213E-05	5.1541E-06
0.8	5.0427E-05	9.6883E-05	7.5204E-06	5.4467E-07	1.1199E-05	5.4431E-06
0.85	6.6698E-05	1.1372E-04	8.8536E-06	7.0160E-07	1.1123E-05	5.2847E-06
0.9	8.7962E-05	1.3335E-04	9.3697E-06	9.4606E-08	1.0878E-05	4.9130E-06
0.95	1.1506E-04	1.5613E-04	9.5236E-06	2.0659E-07	9.5843E-06	4.1418E-06
1	1.4792E-04	1.8247E-04	8.9417E-06	2.0205E-07	6.7054E-06	3.6067E-06

TABLE 8. Statistical form for the dengue model based (A_W) and (S_W) classes.

t	(A_W)			(S_W)		
	Min	Mean	SIR	Min	Mean	SIR
0	3.0060E-07	4.1044E-06	2.2249E-06	5.9308E-07	7.1652E-06	3.3208E-06
0.05	3.5595E-07	5.1307E-06	1.4137E-06	2.6052E-08	5.3058E-06	1.8424E-06
0.1	5.0885E-07	6.6664E-06	2.3319E-06	1.6815E-07	4.7316E-06	2.0576E-06
0.15	6.5754E-07	7.5955E-06	3.7213E-06	3.1043E-07	9.1789E-06	2.8217E-06
0.2	7.3599E-07	7.9459E-06	4.4309E-06	3.0524E-06	1.5063E-05	4.3481E-06
0.25	6.7229E-07	8.1159E-06	3.6385E-06	8.9662E-07	2.0378E-05	7.7740E-06
0.3	5.0286E-07	8.1837E-06	2.4326E-06	2.4110E-07	2.4707E-05	1.0886E-05
0.35	3.0965E-07	8.1917E-06	2.7320E-06	4.2679E-07	2.6959E-05	1.3480E-05
0.4	6.6627E-08	8.3747E-06	4.5958E-06	1.2684E-07	2.6819E-05	1.4697E-05
0.45	8.8853E-08	9.1617E-06	6.0794E-06	1.0298E-06	2.4613E-05	1.3919E-05
0.5	2.6991E-07	1.0275E-05	6.9935E-06	2.6653E-07	2.0617E-05	1.3052E-05
0.55	4.2605E-07	1.1387E-05	7.4624E-06	6.3562E-08	1.5929E-05	1.0371E-05
0.6	3.4533E-08	1.2233E-05	6.5800E-06	8.5327E-07	1.1219E-05	5.0649E-06
0.65	6.2955E-07	1.2915E-05	6.9225E-06	2.2427E-07	7.9768E-06	3.9237E-06
0.7	3.9156E-07	1.3353E-05	6.7272E-06	9.1504E-07	9.0692E-06	4.6328E-06
0.75	2.4959E-08	1.3524E-05	6.1437E-06	1.5198E-06	1.3221E-05	5.5814E-06
0.8	4.2372E-07	1.3201E-05	6.5823E-06	9.1690E-08	1.6045E-05	7.2992E-06
0.85	5.4248E-07	1.2428E-05	7.0547E-06	7.9736E-07	1.7158E-05	7.2016E-06
0.9	4.0630E-07	1.1204E-05	6.8802E-06	1.2240E-06	1.5861E-05	6.0380E-06
0.95	2.2764E-07	9.3822E-06	5.7449E-06	3.5560E-07	1.1748E-05	5.0309E-06
1	8.0483E-09	7.2522E-06	3.9326E-06	5.7371E-08	4.5970E-06	2.9665E-06

TABLE 9. Statistical form for the dengue model based (E_W) and (I_W) classes.

t	(E_W)			(I_W)		
	Min	Mean	SIR	Min	Mean	SIR
0	2.22036068933673e-07	4.55740269105220e-06	2.81025462517057e-06	4.30973995935169e-08	2.19396852703530e-06	1.53890110822161e-06
0.05	6.18705254668006e-08	3.12758782485684e-06	2.77803390168890e-06	1.99001820716527e-08	2.69690746059620e-06	1.33045010846863e-06
0.1	8.62512108679159e-08	3.36078502992804e-06	2.88895797916772e-06	9.22018819904391e-08	3.97175380598483e-06	2.40724890424385e-06
0.15	4.94028725706031e-08	4.68194134068054e-06	1.96802824653855e-06	2.82509819302113e-07	6.09409680109654e-06	3.64424396391214e-06
0.2	1.41536377312734e-07	6.44911819071420e-06	3.18038397158216e-06	7.66144813965641e-07	9.97033965875194e-06	4.72938900709236e-06
0.25	7.08367172003177e-08	8.31549556966418e-06	4.70418892403735e-06	2.44135442427351e-06	1.32180646199416e-05	5.60675552728485e-06
0.3	7.41952215166375e-07	1.01646475519190e-05	4.76086058360387e-06	3.57195298777979e-06	1.53452836494122e-05	9.04327235668953e-06
0.35	6.60289123335933e-07	1.13893451675791e-05	4.62957037290768e-06	1.71520291196436e-06	1.63704146105406e-05	1.06750598916558e-05
0.4	5.53418413123952e-07	1.19475458050432e-05	4.03248311831375e-06	8.74847849247074e-07	1.66388879970190e-05	1.08797981379603e-05
0.45	3.97599815835092e-07	1.23241039415030e-05	3.31504358980911e-06	7.72196147719173e-08	1.59575817948662e-05	1.09022539181748e-05
0.5	1.84286355391083e-07	1.25304332618679e-05	3.68402659661760e-06	1.76063608580551e-06	1.45136350228371e-05	8.96045462660776e-06
0.55	1.14414647846284e-07	1.21839900377979e-05	5.53138083305392e-06	1.94728208258860e-06	1.23825380772453e-05	8.47303178585189e-06
0.6	2.03233698481409e-08	1.13043309435130e-05	5.22910495942032e-06	4.85065860859890e-07	1.01596599801676e-05	6.80307602976896e-06
0.65	7.15506884199635e-07	1.02562708311420e-05	5.06517497191397e-06	4.59354057978645e-07	9.07019588327826e-06	6.06885376842718e-06
0.7	1.37998670678846e-06	8.93627649299622e-06	4.80546180759746e-06	2.54231998467191e-07	7.99206278630574e-06	3.35308269086218e-06
0.75	9.45604892346741e-07	7.41064554232417e-06	4.62076132870005e-06	5.93791905090235e-08	6.95638891492698e-06	4.57931108864378e-06
0.8	4.13881895908186e-07	6.20251523308080e-06	3.80613068615490e-06	2.27567551726315e-07	8.40673494992110e-06	4.53299347690471e-06
0.85	3.44634046252346e-07	6.75760671177451e-06	4.68890659976844e-06	2.91919035437516e-07	9.19251446562276e-06	4.24978184380802e-06
0.9	9.28101204986098e-08	6.75723953484364e-06	4.86213214240944e-06	2.53674047268060e-07	8.53200385312058e-06	4.12755832495358e-06
0.95	3.01514209224973e-08	5.97137549516631e-06	3.49017660701036e-06	1.78503050271561e-07	6.27280924491852e-06	3.34325665435516e-06
1	4.40170110499460e-08	4.05983374677857e-06	2.94002991492980e-06	3.47950698947885e-08	2.55137703230775e-06	2.00388436789878e-06

$$\hat{S}_W(t) = \frac{-0.0038}{1+e^{-(1.6262t-2.6939)}} - \frac{3.7533}{1+e^{-(-1.5112t-3.7917)}} - \frac{0.0323}{1+e^{-(-1.0341t+0.1005)}}, \quad (35)$$

$$\hat{E}_W(t) = \frac{-0.5196}{1+e^{-(1.3278t+1.8181)}} - \frac{0.6266}{1+e^{-(0.2059t+0.2056)}} - \frac{0.4311}{1+e^{-(-.4109t-0.1291)}}, \quad (36)$$

$$\hat{I}_W(t) = \frac{0.0020}{1+e^{-(-12.7782t-3.4483)}} - \frac{1.1030}{1+e^{-(-0.8979t-2.7955)}} - \frac{0.5522}{1+e^{-(-1.3383t-2.6500)}}, \quad (37)$$

Optimization of equation (1) is made through hybrid computing technique GA-ASA by setting 100 runs along 5 neurons. The balance weight of dengue model by GA-ASA are performed and then trained weight along 5 neurons of dengue model is set in Figure 2(i-xiii) for all classes such as S_H, V_H, E_H, I_H, R_H, A_N, S_N, E_N, I_N, A_W, S_W, E_W, and I_W given in equation (1). Figure 3 (i-xiii) constructed the best output of individual class as a result whereas the second half Figure 3 (xiv-xvii) show the comparison result of best weight between GA-ASA with Adam numerical method to solve the dengue model. The visible differences are not seen in all graphs yield close agreement of both strategies. Figure 4 dispatched the Absolute error of proposed model and Adam method where Figure (4a-4m) indicates the AE for S_H in range 10^{-7} to 10^{-5}, for V_H ranging 10^{-6} to 10^{-4}, for E_H in range 10^{-7} to 10^{-5}, I_H in interval 10^{-5} to 10^{-075}, for R_H

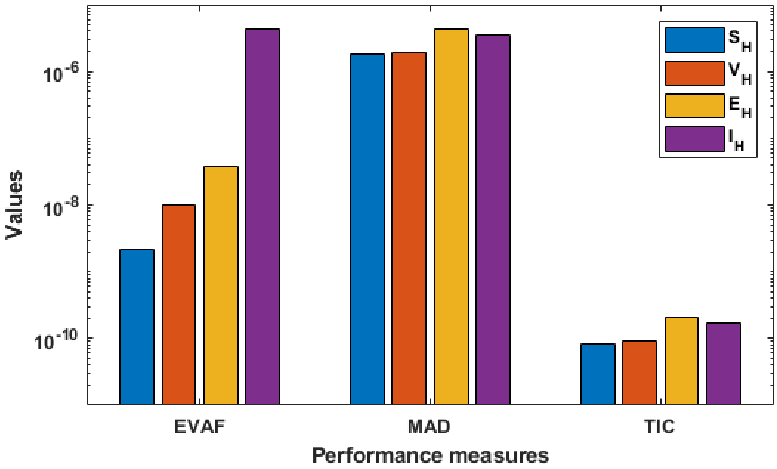

a) Histogram convergence plots for (S_H), (V_H), (E_H), and (I_H) on y-axis.

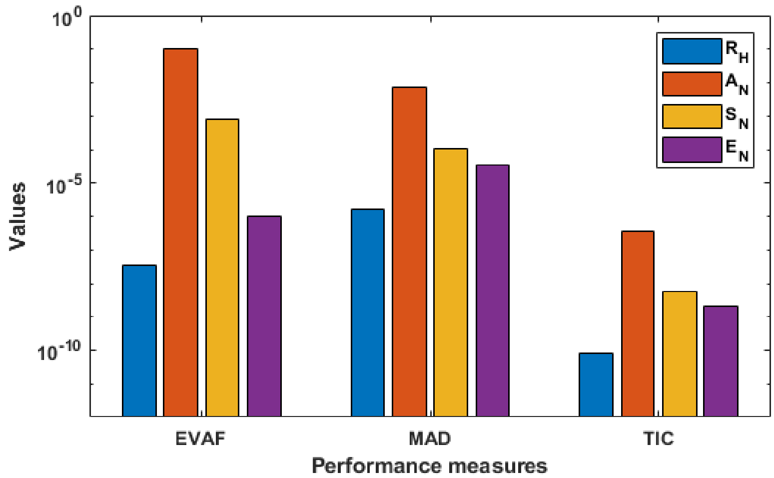

b) Histogram convergence plots for (R_H), (A_N), (S_N), and (E_N) on y-axis.

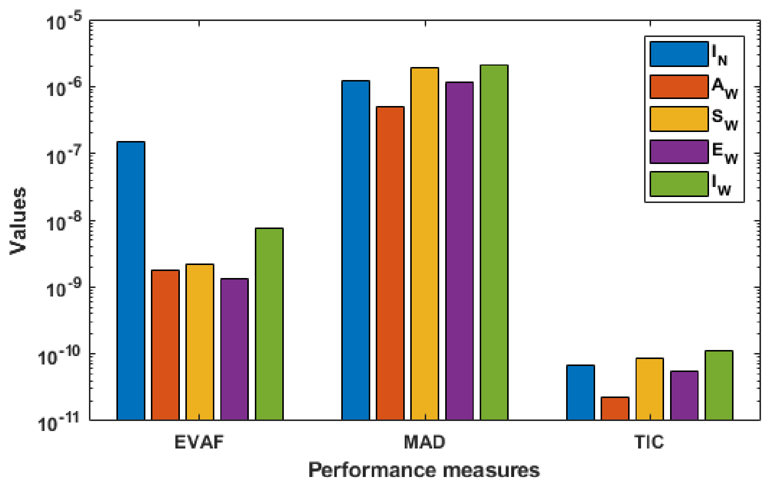

c) Histogram convergence plots for (I_N), (A_W), (S_W), (E_W) and (I_W) on y-axis.

FIGURE 8. **Comparison histogram plots of EVAF, MAD, and TIC for dengue nonlinear model.**

TABLE 10. Global TIC, MAD and E-VAF gages for dengue model.

Class	'G-MAD'		'G-TIC'		'G-EVAF'	
	Min	SIR	Min	SIR	Min	SIR
(S_H)	1.1636E-05	3.7116E-06	5.6555E-10	1.8412E-10	1.2386E-07	8.4516E-08
(V_H)	9.3185E-06	3.4545E-06	4.4188E-10	1.7559E-10	2.5326E-07	2.8162E-07
(E_H)	1.3504E-05	8.0419E-06	6.3888E-10	4.0287E-10	2.8825E-07	4.2281E-07
(I_H)	1.2905E-05	5.7073E-06	6.5340E-10	2.3561E-10	7.5572E-05	4.9109E-05
(R_H)	1.2243E-05	4.3911E-06	5.6940E-10	2.0673E-10	1.3411E-06	8.2096E-07
(A_N)	7.3785E-03	4.8948E-06	3.4929E-07	3.4528E-10	1.0251E-01	4.1984E-04
(S_N)	1.1845E-04	3.2523E-06	6.5360E-09	1.6845E-10	1.1884E-03	7.8390E-05
(E_N)	5.1762E-05	4.1151E-06	2.9793E-09	1.7539E-10	1.8364E-06	2.2532E-07
(I_N)	7.3991E-06	3.7211E-06	3.7317E-10	1.6379E-10	2.8975E-06	2.6266E-06
(A_W)	6.9579E-06	4.0029E-06	3.4331E-10	2.0404E-10	6.8653E-07	6.8112E-07
(S_W)	1.3897E-05	5.3805E-06	6.6657E-10	2.7031E-10	1.6343E-07	1.5222E-07
(E_W)	5.5785E-06	3.6408E-06	2.5119E-10	1.7026E-10	3.1541E-08	5.0920E-08
(I_W)	8.1631E-06	4.5888E-06	3.9105E-10	2.4293E-10	7.6442E-08	1.1903E-07

in range10 $^{-6}$ to 10^{-3}, for A_N in range 10^{-6} to 10^{-3}, for S_N in interval 10^{-6} to 10^{-2}, E_N ranging 10^{-8} to 10^{-4}, for I_N in range 10^{-7} to 10^{-5}, A_W in interval 10^{-8} to 10^{-4}, S_W in 10^{-7} – 10^{-5}, E_W in the range 10^{-7} to 10^{-5}, and I_W in interval 10^{-7} to 10^{-5} proven the resemblance of GA-ASA with numerical Adam method.

Figure 5 (a-c) -7 (a-c) signifies the concert operators built on E-VAF, TIC and MAD to decipher the dengue mathematical model. It is noted that the finest results of S_H, V_H, E_H, and I_H classes with E-VAF, MAD and TIC lie about 10^{-10} to 10^{-2}, 10^{-6} to 10^{-04} and 10^{-10}-10^{-8}, respectively. The good result of R_H, A_N, S_N, and E_N lie around $10^{-8} - 10^{-6}$, $10^{-6} - 10^{-2}$ and $10^{-6} - 10^{-4}$, for these operators, respectively. While, another appropriate results of I_N, A_W, S_W, E_W, and I_W lie around 10^{-9} to 10^{-4}, 10^{-06} to 10^{-4} and 10^{-11} to 10^{-9}, respectively. Since these findings, one might conclude that the proposed strategy is accurate. Figures 8 (a-c) show visualization tools with histograms employing statistical operations to validate the convergence measures for solving the dengue model. Throughout average resemblance of S_H, V_H, E_H, and I_H classes in histogram representation is in the range of 10^{-10} to 10^{-0}, for R_H, A_N, S_N, and E_N in interval 10^{-10} to 10^{-0}, and for I_N, A_W, S_W, E_W, and I_W classes in interval 10^{-11} to 10^{-5} in the case of EVAF, MAD, and TIC declared the convergence region of dengue model via GA-ASA.

Tables 3–8 show statistical analyses for all categories of the dengue mathematics system employing the tools Minimum (Min), Average (Mean), Maximum (Max), Median, SD, SI-Range for highly precise and consistency examination (ST-D).

The better outcomes of the suggested ANN-GA-ASA for handling the dengue mathematical model are the Minimal values whereas the Max values are worth of the suggested ANN-GA-ASA for tackling the dengue model. Based on these proofs of attained results, it is proved that ANN-GA-ASA is reliable and exact.

Convergence tabulation presentation for 100 iterations of ANN-GA-ASA of [G-FIT], [G-MAD], and [G-TIC] tools for each category of dengue model is shown in Table 10. The average values [G-FIT], [G-MAD], and [G-TIC] lie in ranging $10^{-3}-10^{-6}$, $10^{-7}-10^{-10}$, and $10^{-1}-10^{-7}$ whereas SI values in interval $10^{-5} - 10^{-10}$ shows the significance for each category of dengue model. The close optimum outputs were observed by the global evaluations indicate to the ANN-GA-ASA's precision, reliability, and consistency.

V. CONCLUSION

This study is related to design a new coding scheme for tackling the nonlinear dengue mathematical model concern with treatment process. The treatment process is studied for three different situations such as vaccination, Wolbachia therapy, and combine both therapies. Artificial neural networks are used in conjunction with the features of the Genetic algorithm's global and Active-set algorithm as local search methodologies. The dengue nonlinear model is properly tested by manipulating the GA-ASA with neural networks layer structure for 5 number of neurons. The suggested model is tested through overlapping results with Adams numerical technique in the appropriate precision level while simulate the dengue model. Statistical tools in the form of "Mean", "Median", "Semi inter quartile range", "coefficient of Theil's inequality", "Mean absolute deviation", and "Variance account for" reveal the exactness and worth of adopted algorithm. "Mean", and "Semi inter quartile range" operators are used for global significance of nonlinear mathematical dengue model. The MAD and TIC operators are used to calculate the satisfactory values of the performance indices.

REFERENCES

[1] S. B. Tchuandom, J. C. Tchadji, T. F. Tchouangueu, M. Z. Biloa, E. P. Atabonkeng, M. I. M. Fumba, E. S. Massom, G. Nchinda, and J.-R. Kuiate, "A cross-sectional study of acute dengue infection in paediatric clinics in Cameroon," *BMC Public Health*, vol. 19, no. 1, pp. 1–7, Dec. 2019.

[2] B. Kamgang, A. P. Yougang, M. Tchoupo, J. M. Riveron, and C. Wondji, "Temporal distribution and insecticide resistance profile of two major arbovirus vectors Aedes aegypti and Aedes albopictus in Yaoundé, the capital city of Cameroon," *Parasites Vectors*, vol. 10, no. 1, pp. 1–9, 2017.

[3] F. Simard, E. Nchoutpouen, J. C. Toto, and D. Fontenille, "Geographic distribution and breeding site preference of aedes albopictus and Aedes aegypti (diptera: Culicidae) in Cameroon, central Africa," *J. Med. Entomol.*, vol. 42, no. 5, pp. 726–731, Sep. 2005.

[4] A. M. Anand, S. Sistla, R. Dhodapkar, A. Hamide, N. Biswal, and B. Srinivasan, "Evaluation of NS1 antigen detection for early diagnosis of dengue in a tertiary hospital in Southern India," *J. Clin. Diagnostic Res.*, vol. 10, no. 4, pp. DC01–DC04, 2016.

[5] S. Hasan, S. F. Jamdar, M. Alalowi, and S. M. A. A. Al Beaiji, "Dengue virus: A global human threat: Review of literature," *J. Int. Soc. Preventive Community Dentistry*, vol. 6, no. 1, pp. 1–6, 2016.

[6] L. E. Yauch and S. Shresta, "Dengue virus vaccine development," in *Advances in Virus Research*, vol. 88. 2014, pp. 315–372.

[7] Y. Liu, J. Liu, and G. Cheng, "Vaccines and immunization strategies for dengue prevention," *Emerg. Microbes Infections*, vol. 5, no. 1, pp. 1–6, Jan. 2016.

[8] H. Liang, M. Lee, and X. Jin, "Guiding dengue vaccine development using knowledge gained from the success of the yellow fever vaccine," *Cellular Mol. Immunol.*, vol. 13, no. 1, pp. 36–46, Jan. 2016.

[9] N. Khetarpal and I. Khanna, "Dengue fever: Causes, complications, and vaccine strategies," *J. Immunol. Res.*, vol. 2016, Jul. 2016, Art. no. 6803098.

[10] R. Ross, "An Address on the logical basis of the sanitary policy of mosquito reduction: Delivered at the section of preventive medicine of the international congress of arts and science, universal exposition, St. Louis, Sep. 1904," *Brit. Med. J.*, vol. 1, no. 2315, pp. 1025–1029, 1905.

[11] S. A. Carvalho, S. O. da Silva, and I. D. C. Charret, "Mathematical modeling of dengue epidemic: Control methods and vaccination strategies," *Theory Biosci.*, vol. 138, no. 2, pp. 223–239, Nov. 2019.

[12] T. Pang, T. K. Mak, and D. J. Gubler, "Prevention and control of dengue—The light at the end of the tunnel," *Lancet Infectious Diseases*, vol. 17, no. 3, pp. e79–e87, 2017.

[13] M. Umar, M. A. Z. Raja, Z. Sabir, A. S. Alwabli, and M. Shoaib, "A stochastic computational intelligent solver for numerical treatment of mosquito dispersal model in a heterogeneous environment," *Eur. Phys. J. Plus*, vol. 135, no. 7, pp. 1–23, Jul. 2020.

[14] W. Sanusi, N. Badwi, A. Zaki, S. Sidjara, N. Sari, M. I. Pratama, and S. Side, "Analysis and simulation of SIRS model for dengue fever transmission in south Sulawesi, Indonesia," *J. Appl. Math.*, vol. 2021, pp. 1–8, Jan. 2021.

[15] M. Z. Ndii, D. Allingham, R. I. Hickson, and K. Glass, "The effect of Wolbachia on dengue outbreaks when dengue is repeatedly introduced," *Theor. Population Biol.*, vol. 111, pp. 9–15, Oct. 2016.

[16] M. Z. Ndii, D. Allingham, R. I. Hickson, and K. Glass, "The effect of Wolbachia on dengue dynamics in the presence of two serotypes of dengue: Symmetric and asymmetric epidemiological characteristics," *Epidemiol. Infection*, vol. 144, no. 13, pp. 2874–2882, Oct. 2016.

[17] M. Z. Ndii, "Modelling the use of vaccine and Wolbachia on dengue transmission dynamics," *Tropical Med. Infectious Disease*, vol. 5, no. 2, p. 78, 2020.

[18] M. Raffy and A. Tran, "On the dynamics of flying insects populations controlled by large scale information," *Theor. Population Biol.*, vol. 68, no. 2, pp. 91–104, Aug. 2005.

[19] A. Tran and M. Raffy, "On the dynamics of dengue epidemics from large-scale information," *Theor. Population Biol.*, vol. 69, no. 1, pp. 3–12, Feb. 2006.

[20] Z. Sabir, K. Nisar, M. A. Zahoor Raja, M. R. Haque, M. Umar, A. A. Ag Ibrahim, and D.-N. Le, "IoT technology enabled heuristic model with Morlet wavelet neural network for numerical treatment of heterogeneous mosquito release ecosystem," *IEEE Access*, vol. 9, pp. 132897–132913, 2021.

[21] Z. Sabir, M. A. Z. Raja, S. R. Mahmoud, M. Balubaid, A. Algarni, A. H. Alghtani, A. A. Aly, and D.-N. Le, "A novel design of Morlet wavelet to solve the dynamics of nervous stomach nonlinear model," *Int. J. Comput. Intell. Syst.*, vol. 15, no. 1, pp. 1–15, Dec. 2022.

[22] Z. Sabir, M. A. Z. Raja, T. Botmart, and W. Weera, "A neuro-evolution heuristic using active-set techniques to solve a novel nonlinear singular prediction differential model," *Fractal Fractional*, vol. 6, no. 29, pp. 1–14, 2022.

[23] W. Waseem, M. Sulaiman, S. Islam, P. Kumam, R. Nawaz, M. A. Z. Raja, M. Farooq, and M. Shoaib, "A study of changes in temperature profile of porous fin model using cuckoo search algorithm," *Alexandria Eng. J.*, vol. 59, no. 1, pp. 11–24, 2020.

[24] J. Boulent, S. Foucher, J. Théau, and P.-L. St-Charles, "Convolutional neural networks for the automatic identification of plant diseases," *Frontiers Plant Sci.*, vol. 10, pp. 1–15, Jul. 2019.

[25] Z. Sabir, M. Umar, G. M. Shah, H. A. Wahab, and Y. G. Sánchez, "Competency of neural networks for the numerical treatment of nonlinear host-vector-predator model," *Comput. Math. Methods Med.*, vol. 2021, pp. 1–13, Oct. 2021.

[26] M. Umar, Z. Sabir, M. A. Z. Raja, S. Javeed, H. Ahmad, S. K. Elagen, and A. Khames, "Numerical investigations through ANNs for solving COVID-19 model," *Int. J. Environ. Res. Public Health*, vol. 18, no. 22, p. 12192, 2021.

[27] Y. G. Sánchez, Z. Sabir, and J. L. Guirao, "Design of a nonlinear SITR fractal model based on the dynamics of a novel coronavirus (COVID-19)," *Fractals*, vol. 28, no. 8, pp. 1–6, 2020.

[28] M. Umar, Z. Sabir, M. A. Z. Raja, M. Shoaib, M. Gupta, and Y. G. Sánchez, "A stochastic intelligent computing with neuro-evolution heuristics for nonlinear SITR system of novel COVID-19 dynamics," *Symmetry*, vol. 12, no. 10, p. 1628, 2020.

[29] A. Elsonbaty, Z. Sabir, R. Ramaswamy, and W. Adel, "Dynamical analysis of a novel discrete fractional SITRS model for COVID-19," *Fractals*, vol. 29, no. 8, pp. 1–15, Dec. 2021.

[30] M. T. Khan, A. C. Kaushik, L. Ji, S. I. Malik, S. Ali, and D.-Q. Wei, "Artificial neural networks for prediction of tuberculosis disease," *Frontiers Microbiol.*, vol. 10, pp. 1–9, Mar. 2019.

[31] O. Wahyunggoro, A. E. Permanasari, and A. Chamsudin, "Utilization of neural network for disease forecasting," in *Proc. 59th ISI World Statist. Congr.*, vol. 2013, pp. 549–554.

[32] P. N. Srinivasu, J. G. SivaSai, M. F. Ijaz, A. K. Bhoi, W. Kim, and J. J. Kang, ''Classification of skin disease using deep learning neural networks with MobileNet V2 and LSTM,'' *Sensors*, vol. 21, no. 8, p. 2852, 2021.
[33] O. Er, N. Yumusak, and F. Temurtas, ''Chest diseases diagnosis using artificial neural networks,'' *Expert Syst. Appl.*, vol. 37, no. 12, pp. 7648–7655, Dec. 2010.
[34] K. Kumar and B. Abhishek, ''Artificial neural networks for diagnosis of kidney stones disease,'' *Int. J. Inf. Technol. Comput. Sci.*, vol. 4, no. 7, pp. 20–25, 2012.
[35] G. Polezer, Y. S. Tadano, H. V. Siqueira, A. F. Godoi, C. I. Yamamoto, P. A. de André, T. Pauliquevis, M. de Fatima Andrade, A. Oliveira, P. H. Saldiva, and P. E. Taylor, ''Assessing the impact of $PM_{2.5}$ on respiratory disease using artificial neural networks,'' *Environ. Pollut.*, vol. 235, pp. 394–403, Apr. 2018.
[36] Y. Guerrero-Sánchez, M. Umar, Z. Sabir, J. L. Guirao, and M. A. Z. Raja, ''Solving a class of biological HIV infection model of latently infected cells using heuristic approach,'' *Discrete Continuous Dyn. Syst.-S*, vol. 14, no. 10, pp. 3611–3628, 2021.
[37] Z. Sabir, A. A. Ag Ibrahim, M. A. Z. Raja, K. Nisar, M. Umar, J. J. Rodrigues, and S. R. Mahmoud, ''Soft computing paradigms to find the numerical solutions of a nonlinear influenza disease model,'' *Appl. Sci.*, vol. 11, no. 18, p. 8549, 2021.
[38] Y. Guerrero Sánchez, Z. Sabir, H. Günerhan, and H. M. Baskonus, ''Analytical and approximate solutions of a novel nervous stomach mathematical model,'' *Discrete Dyn. Nature Soc.*, vol. 2020, Jul. 2020, Art. no. 5063271.
[39] I. Ahmad, H. Ilyas, A. Urooj, M. S. Aslam, M. Shoaib, and M. A. Z. Raja, ''Novel applications of intelligent computing paradigms for the analysis of nonlinear reactive transport model of the fluid in soft tissues and microvessels,'' *Neural Comput. Appl.*, vol. 31, no. 12, pp. 9041–9059, 2019.
[40] M. Awais, M. A. Z. Raja, S. E. Awan, M. Shoaib, and H. M. Ali, ''Heat and mass transfer phenomenon for the dynamics of Casson fluid through porous medium over shrinking wall subject to Lorentz force and heat source/sink,'' *Alexandria Eng. J.*, vol. 60, no. 1, pp. 1355–1363, 2021.
[41] M. A. Z. Raja, M. F. Malik, C.-L. Chang, M. Shoaib, and C.-M. Shu, ''Design of backpropagation networks for bioconvection model in transverse transportation of rheological fluid involving Lorentz force interaction and gyrotactic microorganisms,'' *J. Taiwan Inst. Chem. Eng.*, vol. 121, pp. 276–291, Apr. 2021.
[42] M. A. Z. Raja, M. Shoaib, Z. Khan, S. Zuhra, C. A. Saleel, K. S. Nisar, S. Islam, and I. Khan, ''Supervised neural networks learning algorithm for three dimensional hybrid nanofluid flow with radiative heat and mass fluxes,'' *Ain Shams Eng. J.*, vol. 13, Mar. 2021, Art. no. 101573.
[43] M. A. Z. Raja, Z. Khan, S. Zuhra, N. I. Chaudhary, W. U. Khan, Y. He, S. Islam, and M. Shoaib, ''Cattaneo-christov heat flux model of 3D Hall current involving biconvection nanofluidic flow with Darcy-Forchheimer law effect: Backpropagation neural networks approach,'' *Case Stud. Therm. Eng.*, vol. 26, Aug. 2021, Art. no. 101168.
[44] J. Horak, J. Vrbka, and P. Suler, ''Support vector machine methods and artificial neural networks used for the development of bankruptcy prediction models and their comparison,'' *J. Risk Financial Manage.*, vol. 13, no. 3, p. 60, 2020.
[45] C. V. Spreckelsen, H.-J. V. Mettenheim, and M. H. Breitner, ''Real-time pricing and hedging of options on currency futures with artificial neural networks,'' vol. 33, pp. 419–432, 2014.
[46] J. H. Holland, *Adaptation in Natural and Artificial Systems: An Introductory Analysis With Applications to Biology, Control, and Artificial Intelligence*. Cambridge, MA, USA: MIT Press, 1992.
[47] A. Vasuki, *Nature-Inspired Optimization Algorithms*. Boca Raton, FL, USA: CRC Press, 2020.
[48] S. Sayed, M. Nassef, A. Badr, and I. Farag, ''A nested genetic algorithm for feature selection in high-dimensional cancer microarray datasets,'' *Expert Syst. Appl.*, vol. 121, pp. 233–243, May 2019.
[49] D. Jude Hemanth and J. Anitha, ''Modified genetic algorithm approaches for classification of abnormal magnetic resonance brain tumour images,'' *Appl. Soft Comput.*, vol. 75, pp. 21–28, Feb. 2019.
[50] H. Motieghader, A. Najafi, B. Sadeghi, and A. Masoudi-Nejad, ''A hybrid gene selection algorithm for microarray cancer classification using genetic algorithm and learning automata,'' *Informat. Med. Unlocked*, vol. 9, pp. 246–254, 2017.
[51] M. Hassoon, M. S. Kouhi, M. Zomorodi-Moghadam, and M. Abdar, ''Rule optimization of boosted C5.0 classification using genetic algorithm for liver disease prediction,'' in *Proc. Int. Conf. Comput. Appl. (ICCA)*, Sep. 2017, pp. 299–305.
[52] M. A. Mohammed, M. K. A. Ghani, R. I. Hamed, S. A. Mostafa, M. S. Ahmad, and D. A. Ibrahim, ''Solving vehicle routing problem by using improved genetic algorithm for optimal solution,'' *J. Comput. Sci.*, vol. 21, pp. 255–262, Jul. 2017.
[53] Y. Jiang, P. Wu, J. Zeng, Y. Zhang, Y. Zhang, and S. Wang, ''Multi-parameter and multi-objective optimisation of articulated monorail vehicle system dynamics using genetic algorithm,'' *Vehicle Syst. Dyn.*, vol. 58, no. 1, pp. 74–91, Jan. 2020.
[54] D. Jahed Armaghani, M. Hasanipanah, A. Mahdiyar, M. Z. Abd Majid, H. Bakhshandeh Amnieh, and M. M. D. Tahir, ''Airblast prediction through a hybrid genetic algorithm-ANN model,'' *Neural Comput. Appl.*, vol. 29, no. 9, pp. 619–629, May 2018.
[55] Y. Yang, B. Yang, S. Wang, F. Liu, Y. Wang, and X. Shu, ''A dynamic ant-colony genetic algorithm for cloud service composition optimization,'' *Int. J. Adv. Manuf. Technol.*, vol. 102, nos. 1–4, pp. 355–368, 2019.
[56] S. M. Seyedpour, P. Kirmizakis, P. Brennan, R. Doherty, and T. Ricken, ''Optimal remediation design and simulation of groundwater flow coupled to contaminant transport using genetic algorithm and radial point collocation method (RPCM),'' *Sci. Total Environ.*, vol. 669, pp. 389–399, Jun. 2019.
[57] J.-C. Lee, W.-M. Lin, G.-C. Liao, and T.-P. Tsao, ''Quantum genetic algorithm for dynamic economic dispatch with valve-point effects and including wind power system,'' *Int. J. Electr. Power Energy Syst.*, vol. 33, no. 2, pp. 189–197, Feb. 2011.
[58] O. Piller, S. Elhay, J. W. Deuerlein, and A. R. Simpson, ''A content-based active-set method for pressure-dependent models of water distribution systems with flow controls,'' *J. Water Resour. Planning Manage.*, vol. 146, no. 4, Apr. 2020, Art. no. 04020009.
[59] M. Azizi, M. Amirfakhrian, and M. A. F. Araghi, ''A fuzzy system based active set algorithm for the numerical solution of the optimal control problem governed by partial differential equation,'' *Eur. J. Control*, vol. 54, pp. 99–110, Jul. 2020.
[60] I. Antonau, M. Hojjat, and K.-U. Bletzinger, ''Relaxed gradient projection algorithm for constrained node-based shape optimization,'' *Struct. Multidisciplinary Optim.*, vol. 63, no. 4, pp. 1633–1651, Apr. 2021.
[61] S. Abide, M. Barboteu, S. Cherkaoui, D. Danan, and S. Dumont, ''Inexact primal–dual active set method for solving elastodynamic frictional contact problems,'' *Comput. Math. Appl.*, vol. 82, pp. 36–59, Jan. 2021.

PREM JUNSAWANG received the B.Sc. degree (Hons.) in mathematics from Khon Kaen University, Khon Kaen, Thailand, in 2004, and the M.Sc. degree in computational science and the Ph.D. degree in computer science from Chulalongkorn University, Bangkok, Patumwan, Thailand, in 2008 and 2018, respectively. He is currently a Lecturer at the Department of Statistics, Faculty of Science, Khon Kaen University. His research interests include artificial neural networks, synchronization, pattern recognition, data mining, and machine learning.

SAMINA ZUHRA received the M.Sc. degree in mathematics from the University of Peshawar, Pakistan, in 2008, the M.Phil. degree from the Islamia College Peshawar, Pakistan, and the Ph.D. degree from Abdul Wali Khan University Mardan, Pakistan, in 2019. She has published many research articles in international journals with impact factor. Her research interests include solving differential system via numerical and semi-analytical techniques, fluidic, and nanofluids.

ZULQURNAIN SABIR was born in Pothi, Jhelum, Pakistan. He received the M.Sc. degree in mathematics from Punjab University, Lahore, Pakistan, and the M.Phil. degree in mathematics from Preston University Kohat, Islamabad Campus, Pakistan. He is currently pursuing the Ph.D. degree in mathematics from Hazara University, Mansehra, Pakistan. He has published more than 80 research articles in reported international WoS journals with impact factors. His research interests include mathematical modeling, unsupervised/supervised neural networks, artificial intelligence, mathematical modeling, and implementation of computational-based traditional as well as heuristic techniques. He is famous for solving singular nonlinear, functional, fractional, higher-order, biological, and fluid models. He is a pioneer in designing and solving the second-order pantograph Emden-Fowler model, prediction differential model, nonlinear fifth, sixth, and seven order Emden-Fowler model. He also designed the nonlinear multi-singular SITR model based on coronavirus (COVID 19), nervous stomach, and prediction differential model.

MUHAMMAD ASIF ZAHOOR RAJA was born in Muhallah Sadiqabad, Rawalpindi, Pakistan. He received the M.Sc. degree in mathematics from the Forman Christen College, Lahore, Pakistan, in 1996, the M.Sc. degree in nuclear engineering from Quaid-e-Azam, University, Islamabad, Pakistan, in 1999, and the Ph.D. degree in electronic engineering from International Islamic University, Islamabad, in 2011. He was involved in research and development assignments of the Engineering and Scientific Commission of Pakistan, from 1999 to 2012. He is currently working as an Assistant Professor with the Department of Electrical Engineering, COMSATS Institute of Information Technology, Attock Campus, Attock, Pakistan, and also associated with the Future Technology Research Center, National Yunlin University of Science and Technology, Douliou, Yunlin, Taiwan, for the research work. He has developed the fractional least mean square algorithm, and the computational platform is formulated for the first time for solving fractional differential equations using artificial intelligence techniques during his Ph.D. studies. He has been the author of more than 250 publications, out of which more than 220 are reputed journal publications with an impact factor of more than 700. He acts as a resource person and gives invited talks on many workshops and conferences held at the national level. His research interests include solving linear and nonlinear differential equations of arbitrary order, active noise control systems, fractional adaptive signal processing, nonlinear system identification, the direction of arrival estimation, and bioinformatics problems.

MUHAMMAD SHOAIB was born in Basal, Attock, Punjab, Pakistan. He received the master's and Ph.D. degrees in mathematics from Riphah International University, Islamabad, Pakistan, in 2012 and 2016, respectively. Since 2017, he has been working as an Assistant Professor with COMSATS University Islamabad, Attock Campus. He has about 120 research publications with impact factor more than 380 in international journals. His research interests include mathematical modeling, neural networks, artificial intelligence, and implementation of computational techniques based on traditional as well as the heuristic paradigms on the problems arise in the fields of fluid dynamics, information technology, mathematical physics, environmental science, economics, finance, and bioinformatics. He is already working on different research projects in collaboration with national as well as international research institutes. He also works as a resource person and gives invited talks on seminars and conferences held at the national and international level.

THONGCHAI BOTMART received the B.S. degree in mathematics from Khon Kaen University, Khon Kaen, Thailand, in 2002, and the M.S. degree in applied mathematics and the Ph.D. degree in mathematics from Chiang Mai University, Chiang Mai, Thailand, in 2005 and 2011, respectively. He is currently an Associate Professor with the Department of Mathematics, Faculty of Science, Khon Kaen University. His research interests include stability theory of time-delay systems, non-autonomous systems, switched systems, artificial neural networks, complex dynamical networks, synchronization, control theory, and chaos theory.

WAJAREE WEERA received the B.S. degree in mathematics, the M.S. degree in applied mathematics, and the Ph.D. degree in mathematics from Chiang Mai University, Chiang Mai, Thailand, in 2005, 2007, and 2015, respectively. She is currently an Assistant Professor with the Department of Mathematics, Faculty of Science, Khon Kaen University. Her research interests include stability theory of time-delay systems, stability analysis, neutral systems, switched systems, and artificial neural networks.